



US007983737B2

(12) **United States Patent**
Feldman et al.

(10) **Patent No.:** **US 7,983,737 B2**
(45) **Date of Patent:** ***Jul. 19, 2011**

(54) **OPTICAL COHERENCE TOMOGRAPHIC
DETECTION OF CELLS AND
COMPOSITIONS**

(75) Inventors: **Marc D. Feldman**, San Antonio, TX
(US); **Thomas E. Milner**, Austin, TX
(US); **Jung-Hwan Oh**, Austin, TX (US);
Mehmet Cilingeroglu, Little Rock, TX
(US)

2003/0055307	A1	3/2003	Elmaleh et al.	600/1
2004/0023415	A1	2/2004	Sokolov et al.	
2004/0098070	A1 *	5/2004	Mohr et al.	607/89
2004/0239942	A1	12/2004	Sun	356/479
2004/0254419	A1	12/2004	Wang et al.	600/8
2004/0258759	A1	12/2004	Suslick et al.	424/490
2005/0165298	A1	7/2005	Larson et al.	600/410
2005/0171433	A1	8/2005	Boppart et al.	600/473
2005/0203424	A1	9/2005	Boese et al.	600/478

(Continued)

(73) Assignee: **Board of Regents, The University of
Texas Systems**, Austin, TX (US)

FOREIGN PATENT DOCUMENTS

WO WO 96/23524 2/1996

(Continued)

(*) Notice: Subject to any disclaimer, the term of this
patent is extended or adjusted under 35
U.S.C. 154(b) by 962 days.

This patent is subject to a terminal dis-
claimer.

OTHER PUBLICATIONS

Cilingeroglu, et al., "Detection of Vulnerable Plaque in a Murine
Model of Atherosclerosis With Optical Coherence Tomography,"
Catheterization and Cardiovascular Interventions, 67:915-923
(2006).

(21) Appl. No.: **11/441,824**

(22) Filed: **May 26, 2006**

(Continued)

(65) **Prior Publication Data**

US 2007/0038121 A1 Feb. 15, 2007

Related U.S. Application Data

(60) Provisional application No. 60/685,559, filed on May
27, 2005.

(51) **Int. Cl.**
A61B 6/00 (2006.01)

(52) **U.S. Cl.** **600/476**

(58) **Field of Classification Search** **600/407,**
600/473, 476

See application file for complete search history.

(56) **References Cited**

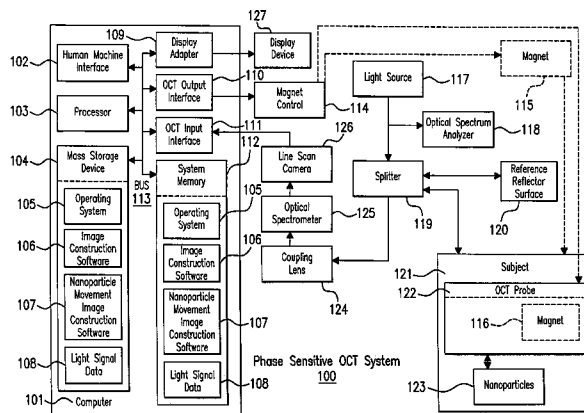
U.S. PATENT DOCUMENTS

6,795,195	B1	9/2004	Barbour et al.	356/446
2002/0190212	A1	12/2002	Boas et al.	250/341.1
2002/0193785	A1	12/2002	Naghavi et al.	606/28

(57) **ABSTRACT**

Provided herein are systems and methods for the detection of
cells and/or compositions using optical coherence tomogra-
phy. The systems and methods comprise a plurality of mag-
nets for applying a plurality of distinct magnetic field
strengths to the cells and/or compositions and a phase sensi-
tive optical coherence tomographic imaging modality for
detecting the cells and/or compositions while same are dis-
posed in the presence of at least one of the plurality of distinct
magnetic field strengths.

71 Claims, 18 Drawing Sheets



U.S. PATENT DOCUMENTS

2005/0256207	A1	11/2005	McGrath	514/673
2006/0256343	A1	11/2006	Choma et al.	356/450
2007/0038121	A1	2/2007	Feldman et al.	600/476
2007/0260138	A1 *	11/2007	Feldman et al.	600/409
2008/0095714	A1 *	4/2008	Castella et al.	424/9.3
2008/0097185	A1 *	4/2008	Feldman et al.	600/407
2008/0097194	A1 *	4/2008	Milner	600/425
2008/0154128	A1 *	6/2008	Milner	600/427
2009/0043198	A1 *	2/2009	Milner et al.	600/437

FOREIGN PATENT DOCUMENTS

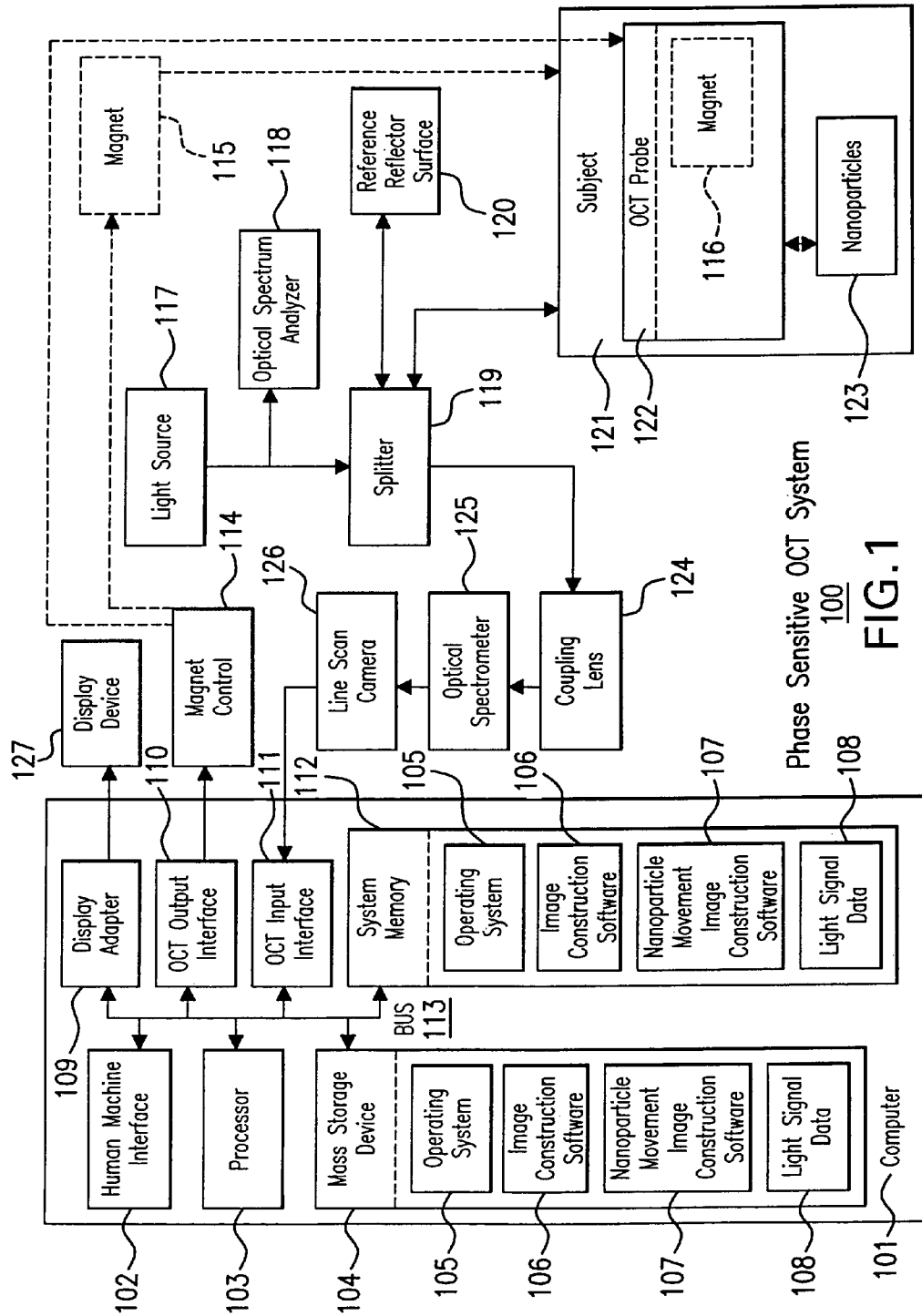
WO	WO 99/13916	3/1999
WO	WO 2004/096049	4/2004

OTHER PUBLICATIONS

Elghanian, R., et al., Selective Colorimetric Detection of Polynucleotides Based On The Distance-Dependent Optical Properties Of Gold Nanoparticles. *Science*, 277(5329): 1078-1080 (1997).
 Kelly et al., "Detection of Vascular Adhesion Molecule-1 Expression Using a Novel Multimodal Nanoparticle," *Circulation Res.*, 96:327-336 (2005).
 Lee et al., "Engineered microsphere contrast agents for optical coherence tomography," *Optics Letters* 28(17) 1546-1548 (2003).
 Loo et al., "Nanoshell-Enabled Photonics-Based Imaging and Therapy of Cancer," *Tech. Cancer Res. and Treatment*, 3(1) 33-40 (2004).
 Mindlin, "Force at a Point in the Interior of a Semi-Infinite Solid," *Physics*, 7:195-202 (1936).

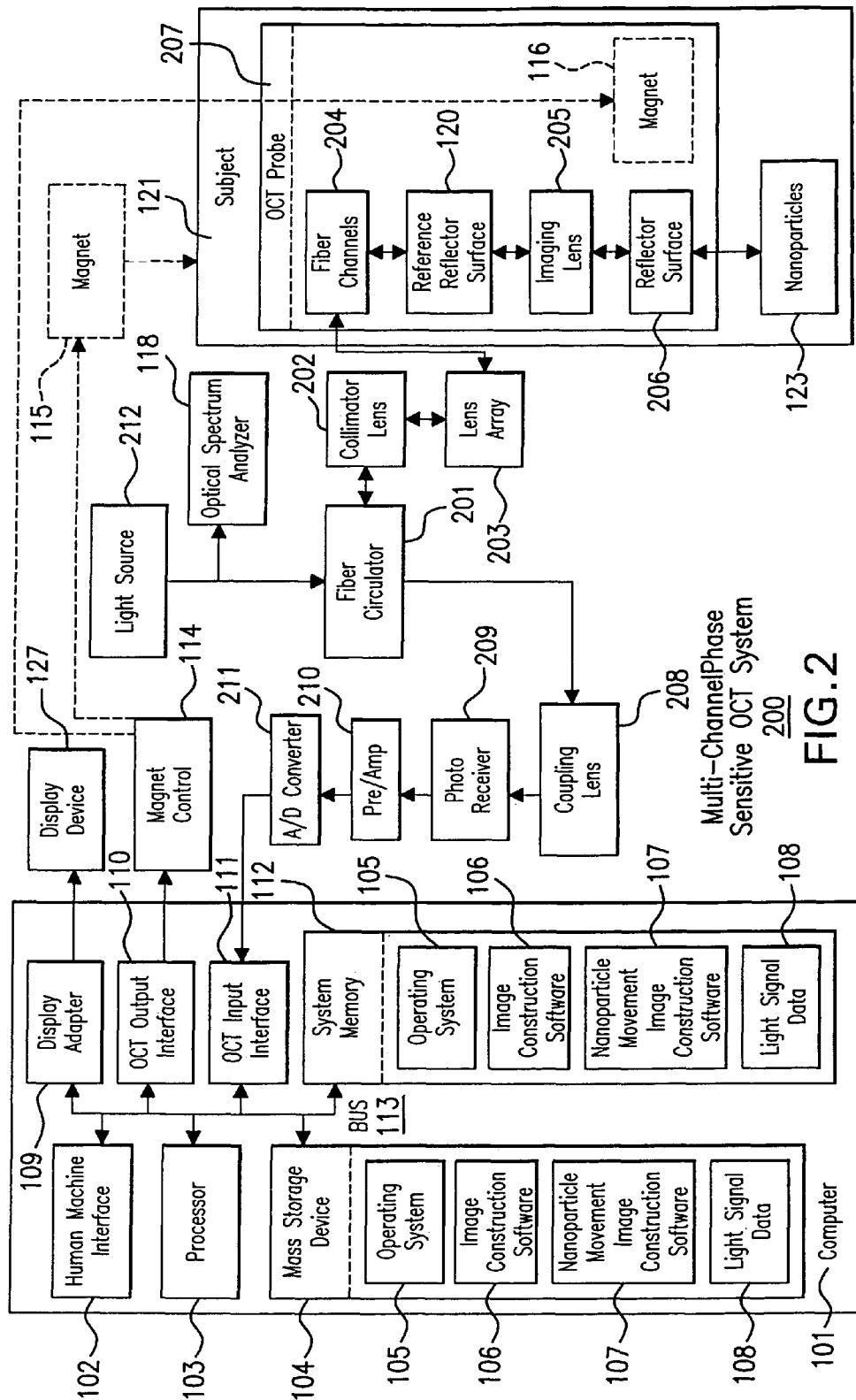
Nakamura et al., "Identification and Treatment of Vulnerable Plaque," *Rev. in Cardiovascular Med.*, 5(Suppl. 2):S22-S33 (2004).
 Oh, et al., "Detection of Magnetic Nanoparticles in Tissue Using Magneto-Motive Ultrasound," *Nanotechnology* 7:4183-4190 (2006).
 Oh, et al., "Magneto-Motive Detection of Tissue-Based Macrophages by Differential Phase Optical Coherence Tomography," *Lasers in Surgery and Medicine*, Wiley-Liss, Inc. 1-5 (2007).
 Oldenburg et al., "Magnetic contrast agents for optical coherence tomography," *Proc. SPIE* 5316 26-28 (2004).
 Oldenburg et al., "Nanoengineering of Optical Resonances," *Chemical Physics Letters* 288, 243-247 (1998).
 Regar et al., "Optical Coherence Tomography," *Cardiovascular Rad. Med.*, 4 198-204 (2003).
 Robles, "Short-Duration High-Frequency Quasi-Sinusoidal Magnetic Field Generator," *IEEE Transactions On Instrumentation And Measurement*, vol. 54, No. 6:2481-2485 (Dec. 2005).
 Sirol et al., "Molecular Imaging for the Diagnosis of High-Risk Plaque," *Cardiovascular Res.*, 96(12) 1219-1224 (2003).
 Tearney et al., "Quantification of Macrophage Content in Atherosclerotic Plaques by Optical Coherence Tomography," *Circulation*, 107:113-119 (2003).
 Villard, et al., "Use of a Blood Substitute to Determine Instantaneous Murine Right Ventricular Thickening With Optical Coherence Tomography," *Circulation: Journal of the American Heart Association*, 105:1843-1849 (2002).
 International Search Report, pp. 1-3 (Mar. 2008).
 International Search Report, pp. 1-4 (Feb. 2009).
 Publication of International Search Report, pp. 1-2 (Nov. 30, 2006).

* cited by examiner



Phase Sensitive OCT System

FIG. 1



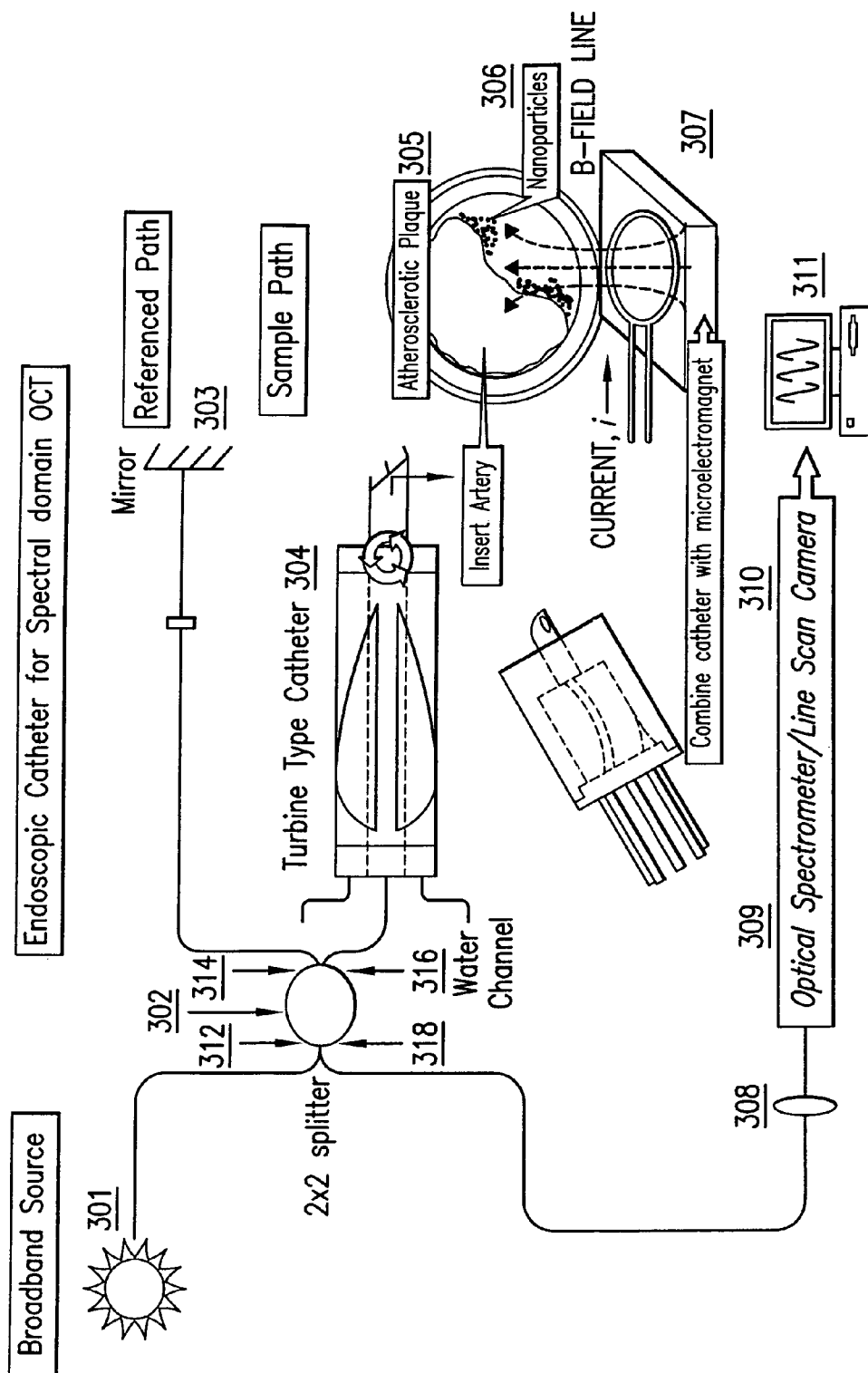


FIG.3

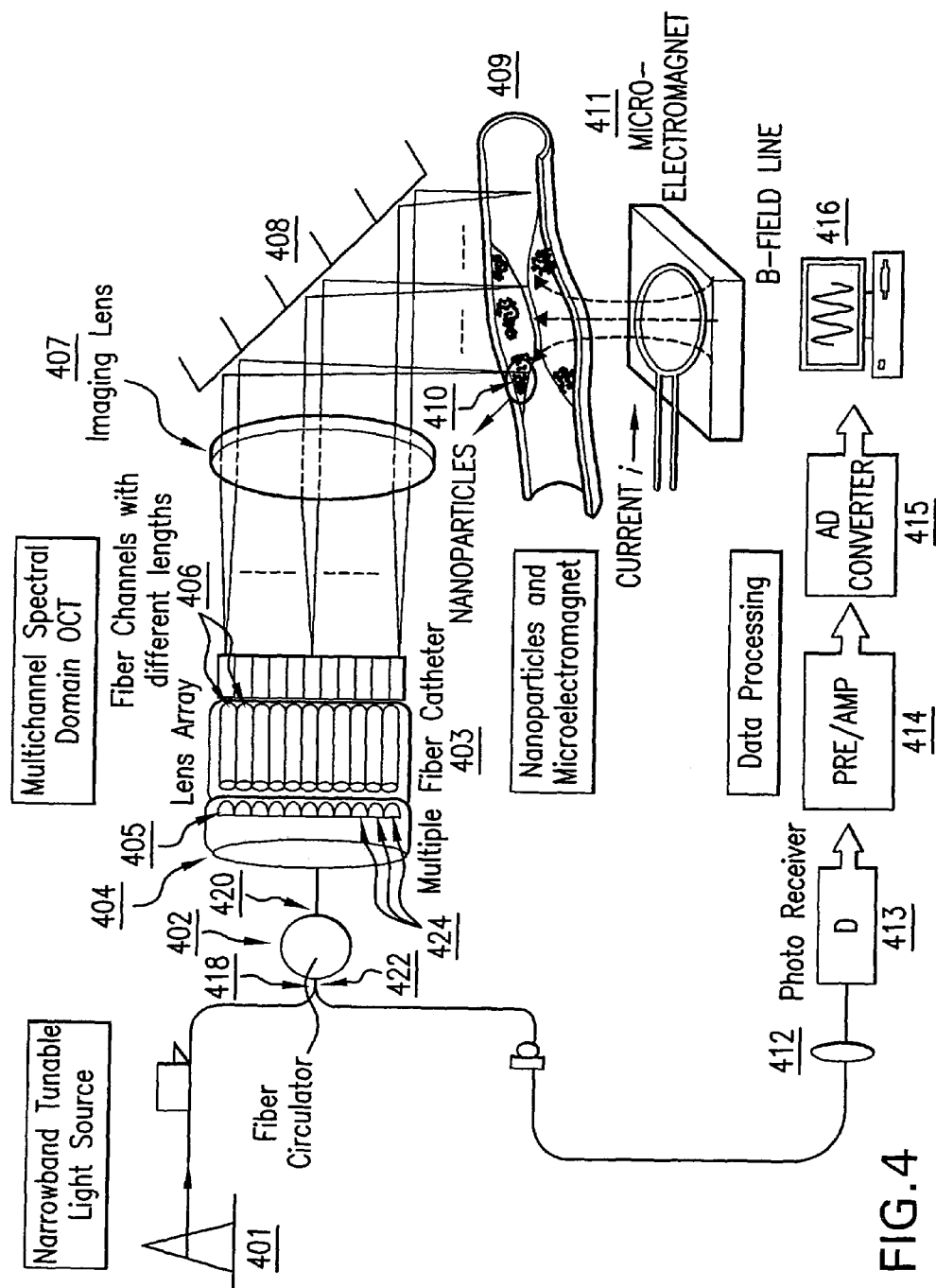


FIG. 4

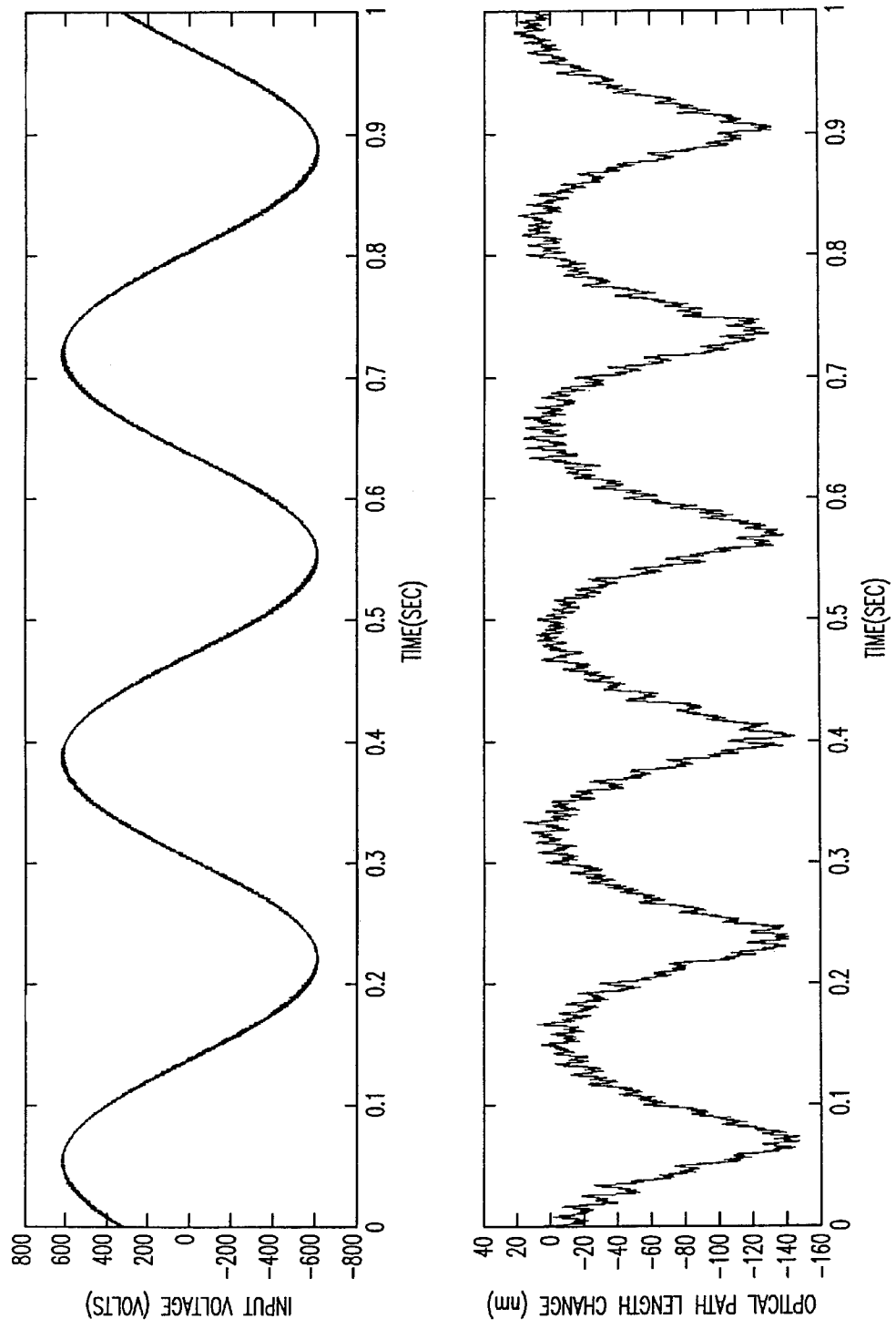


FIG.5A

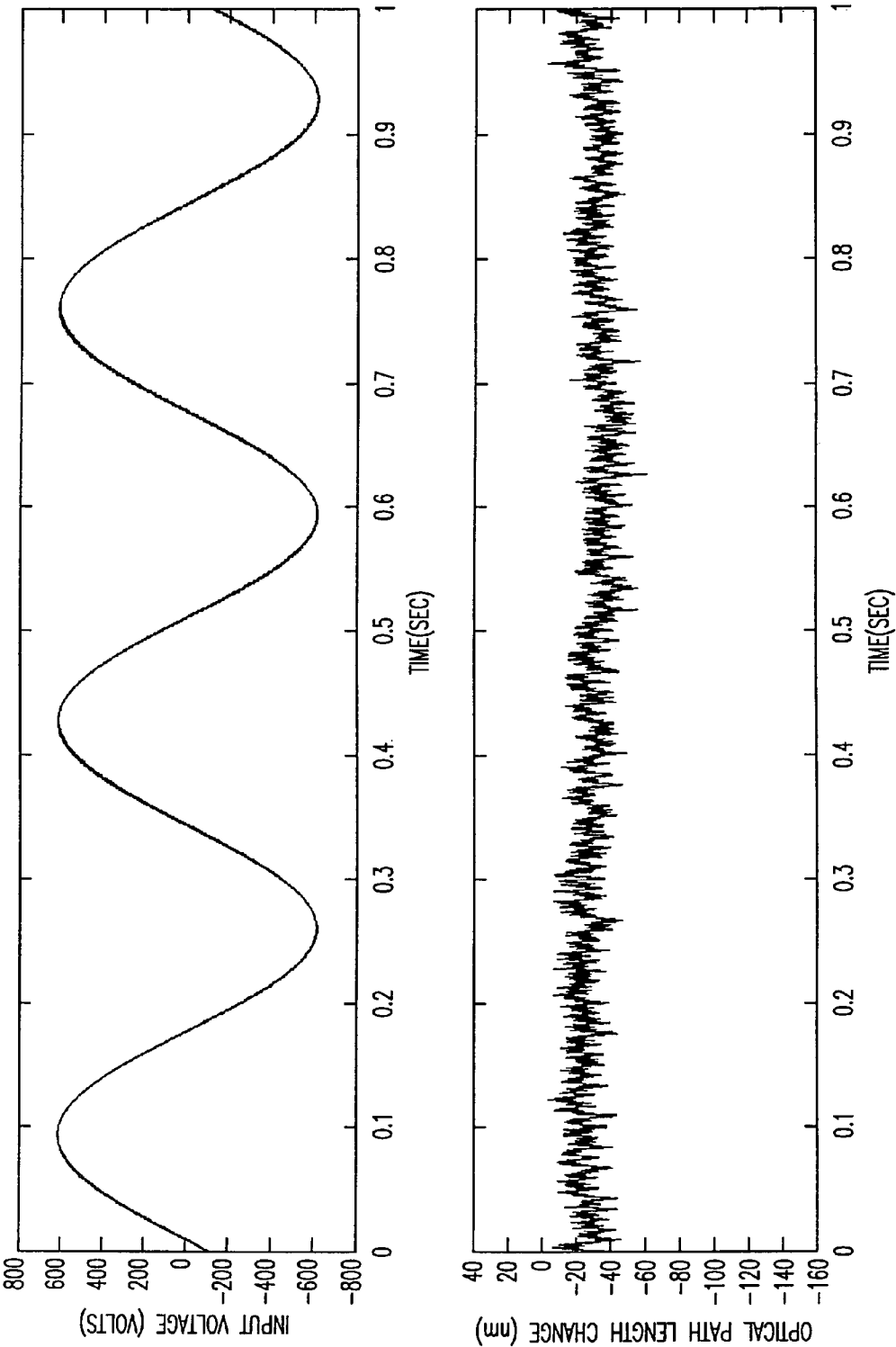


FIG. 5B

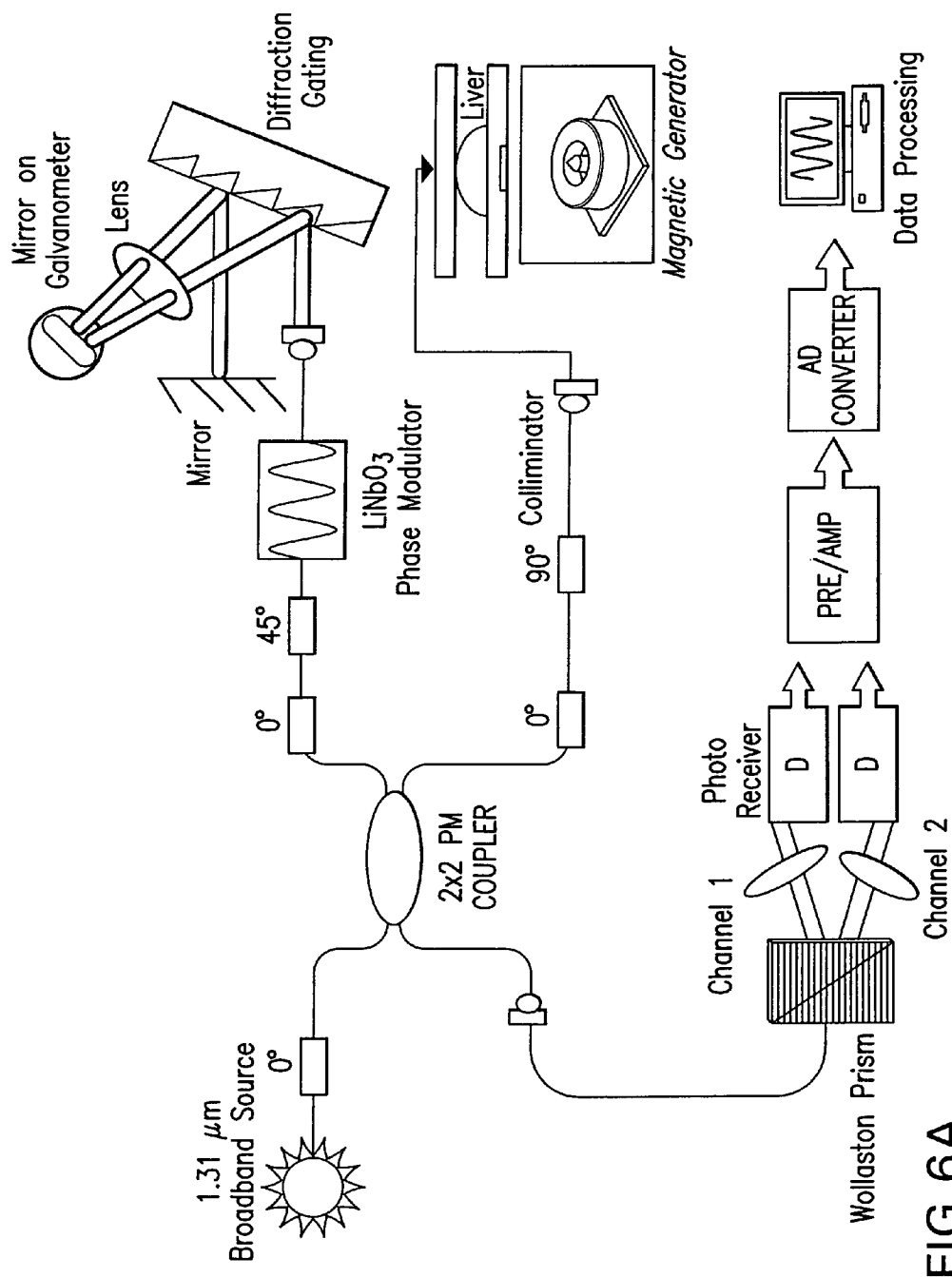


FIG. 6A

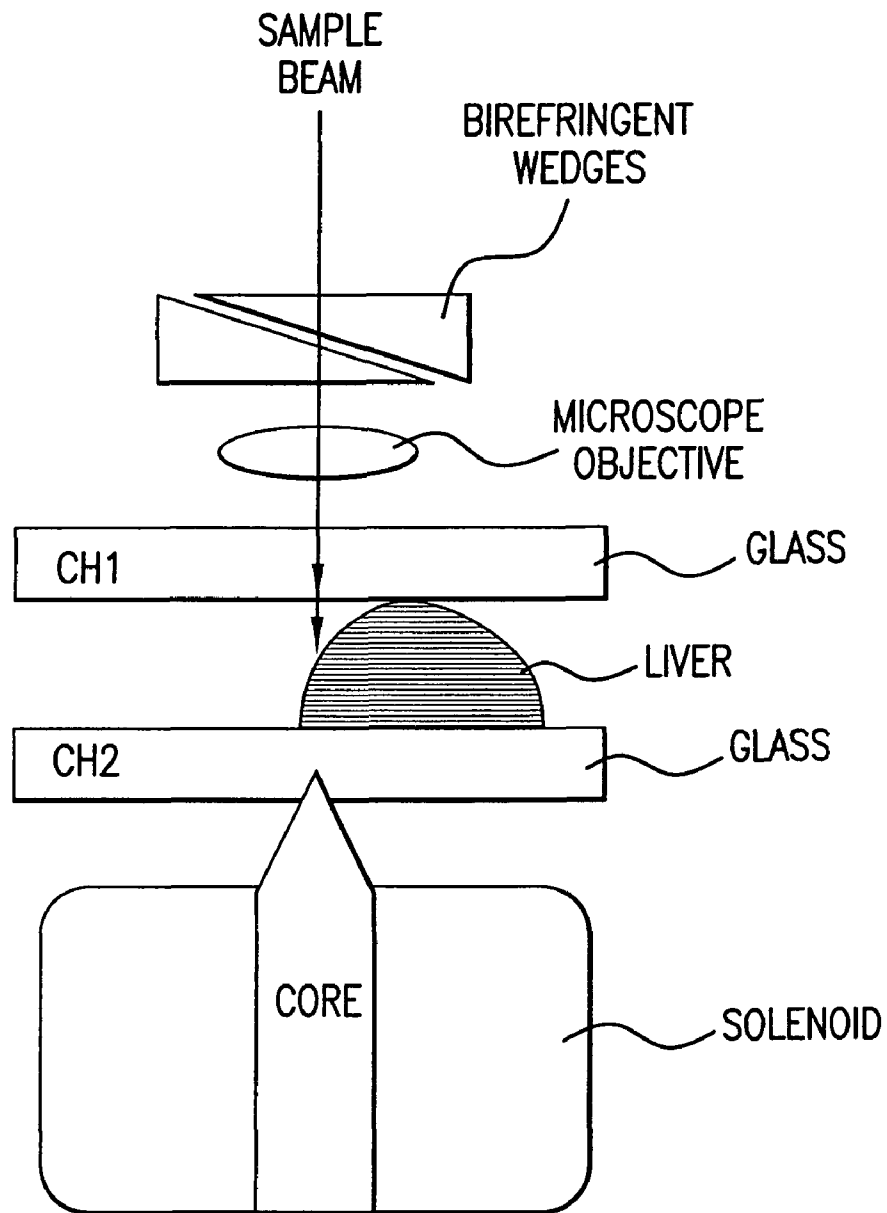


FIG. 6B

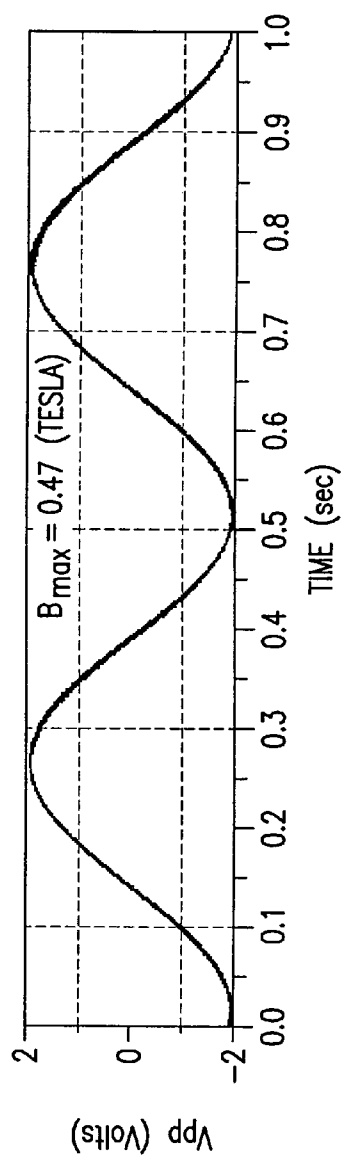


FIG. 7A

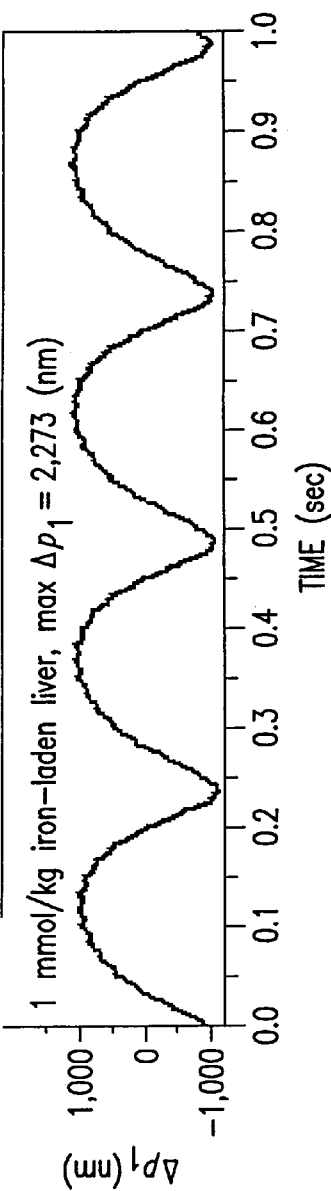


FIG. 7B

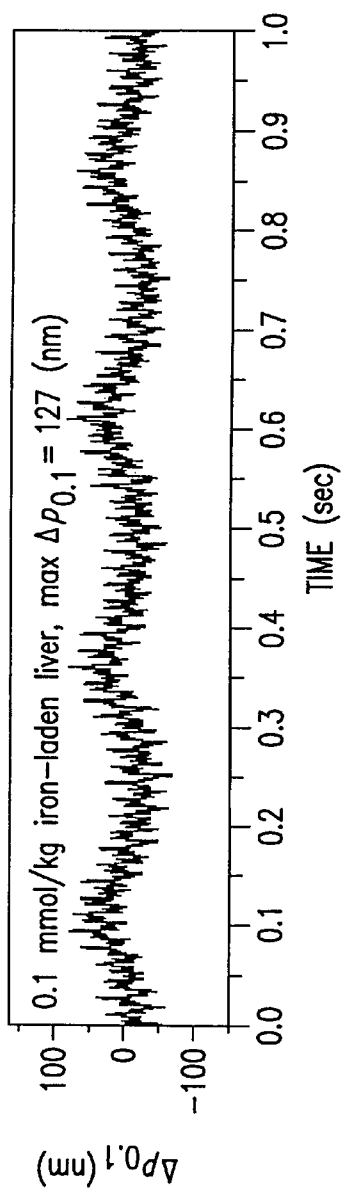


FIG. 7C

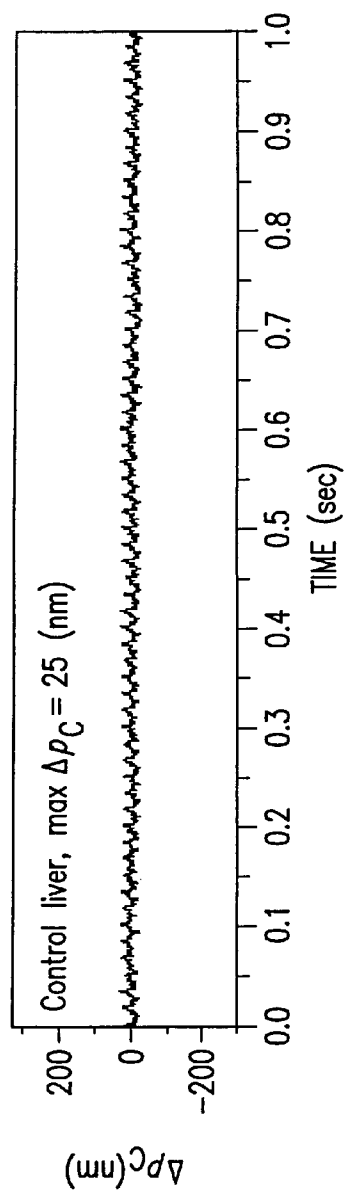


FIG. 7D

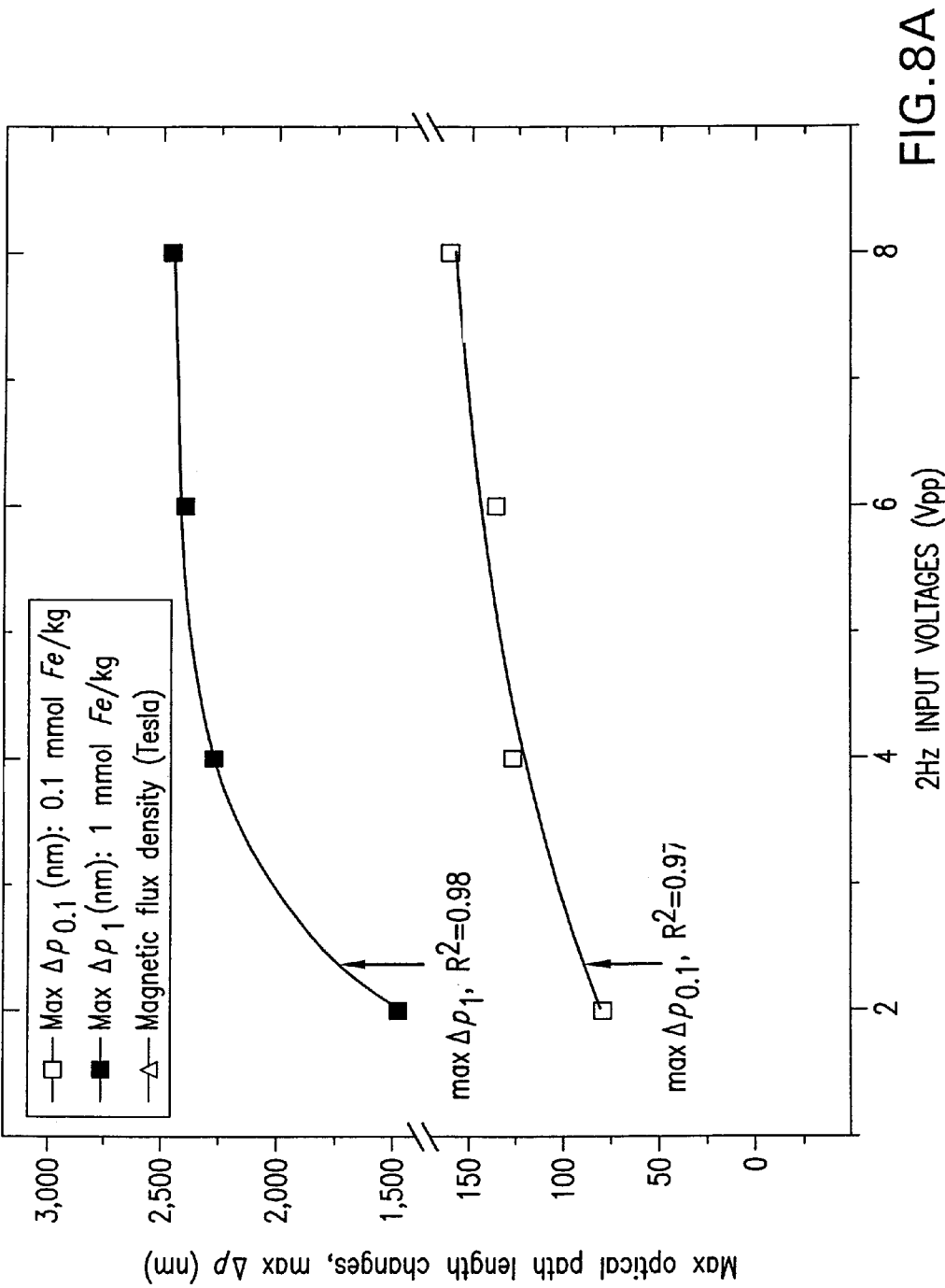


FIG. 8A

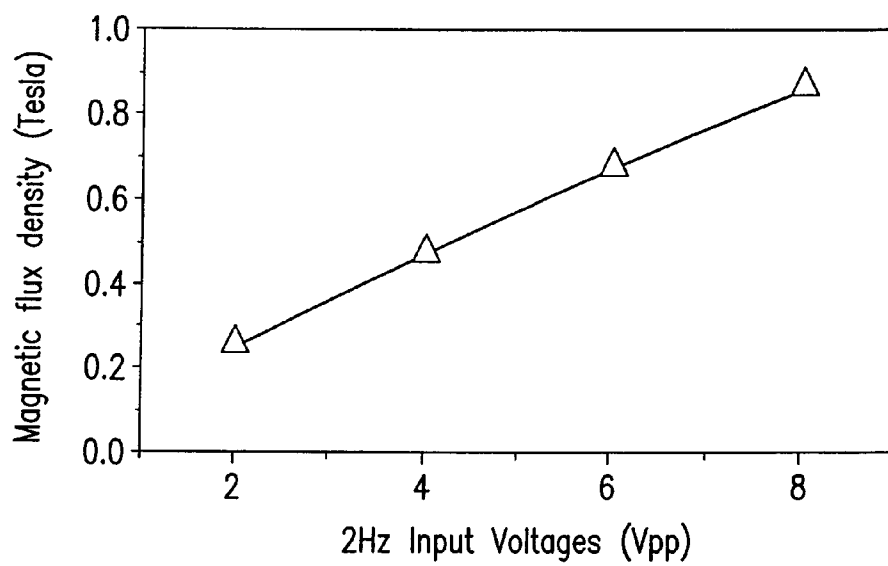


FIG.8B

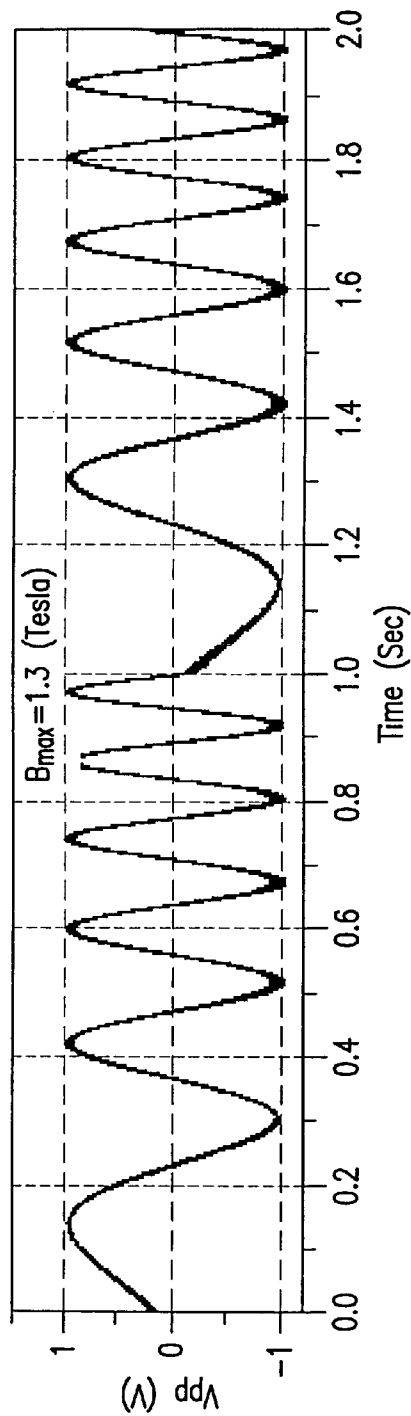


FIG. 9A

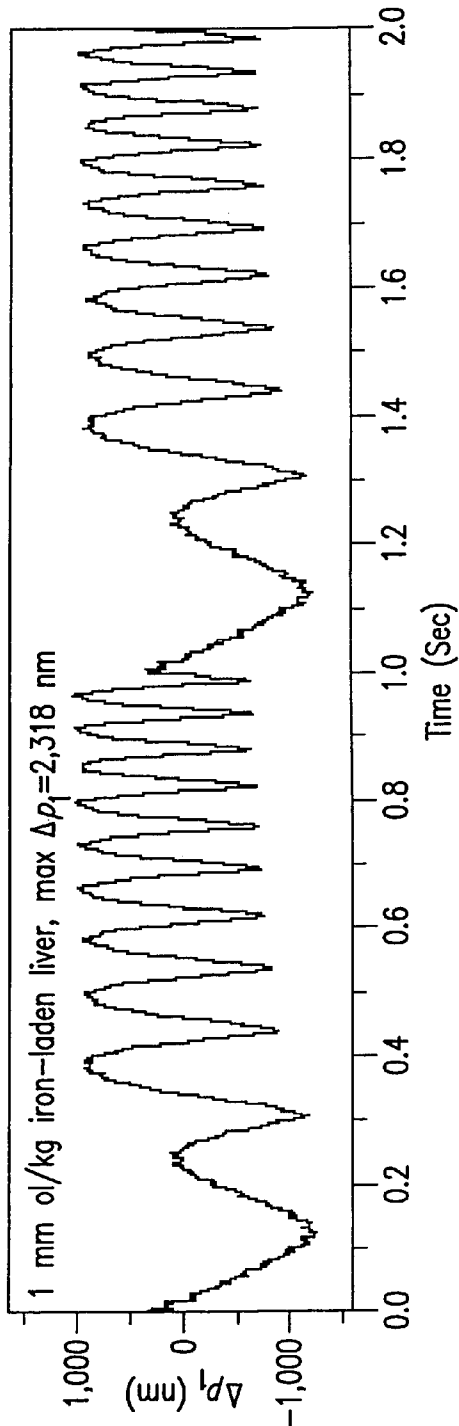


FIG. 9B

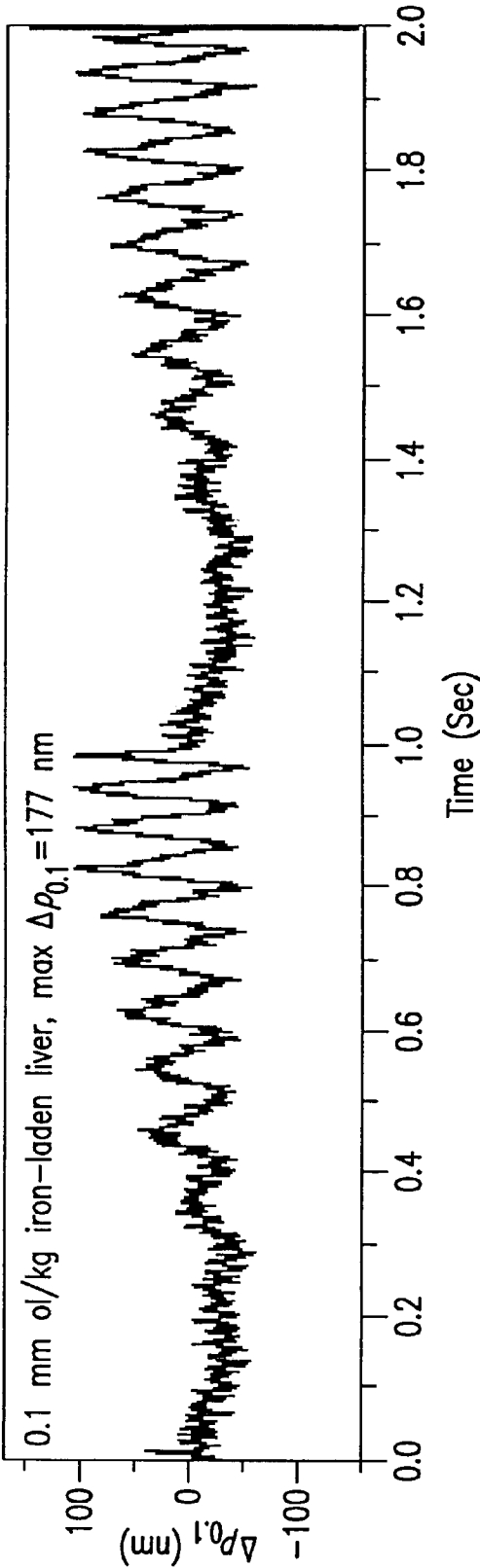


FIG.9C

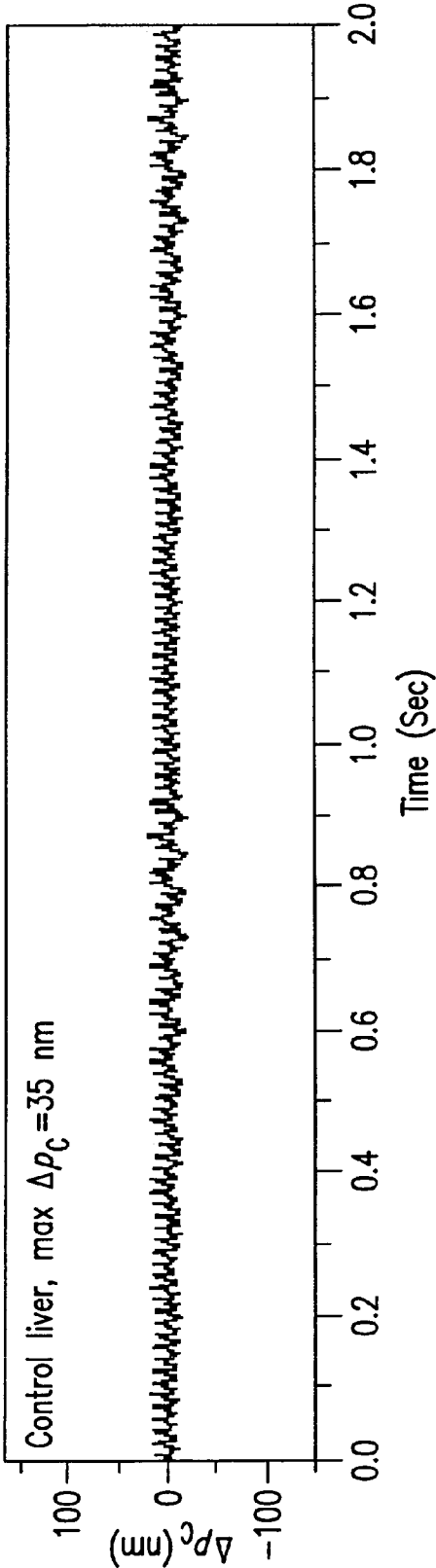


FIG.9D

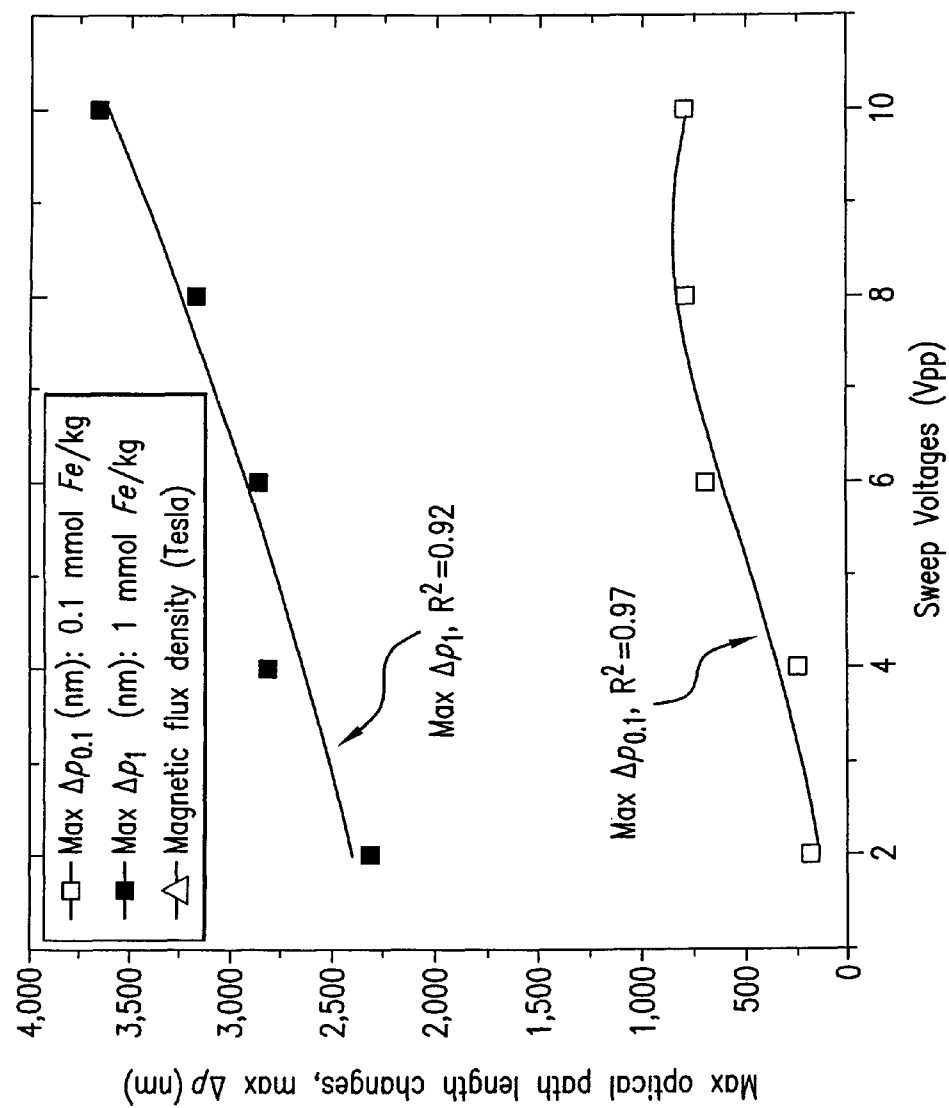


FIG. 10A

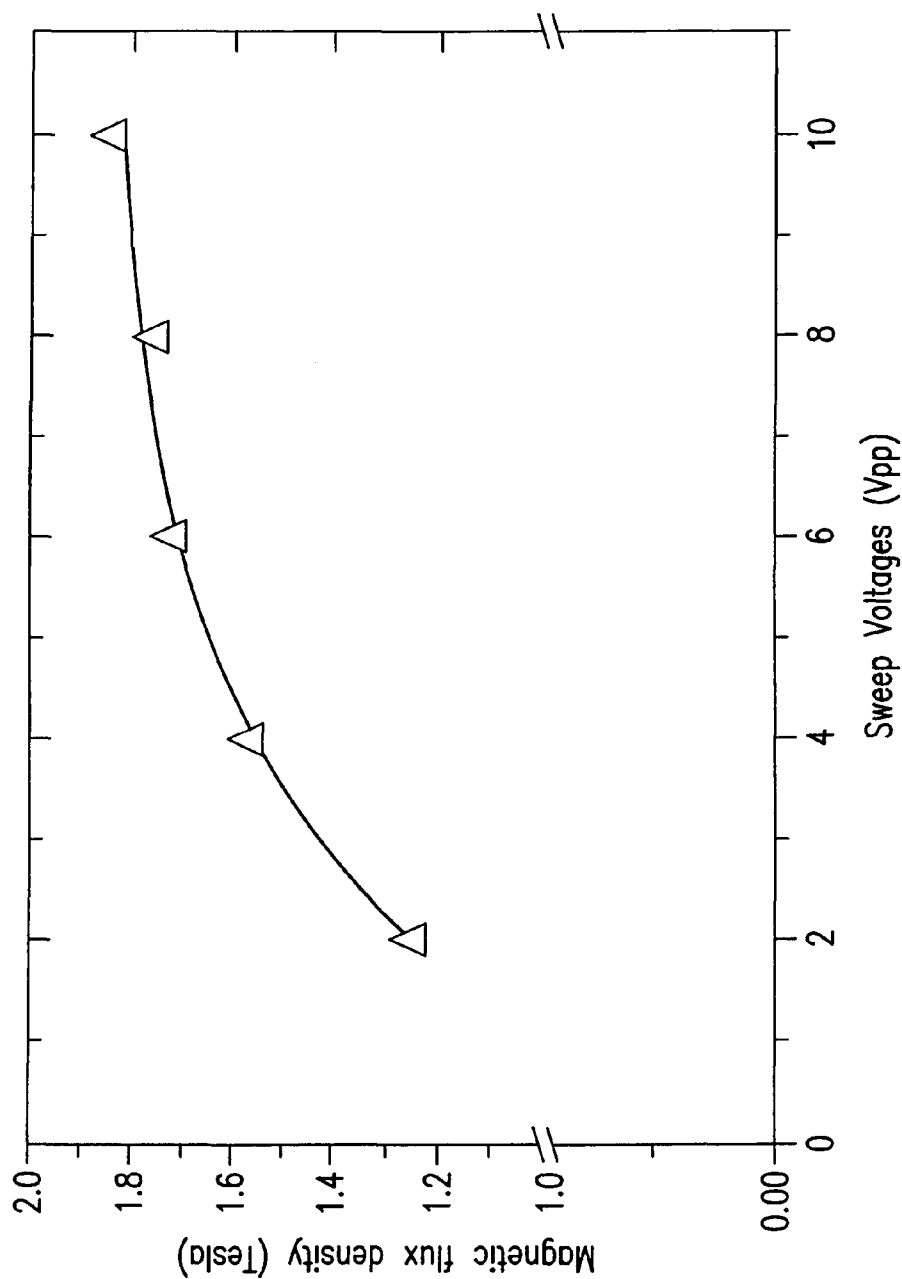


FIG.10B

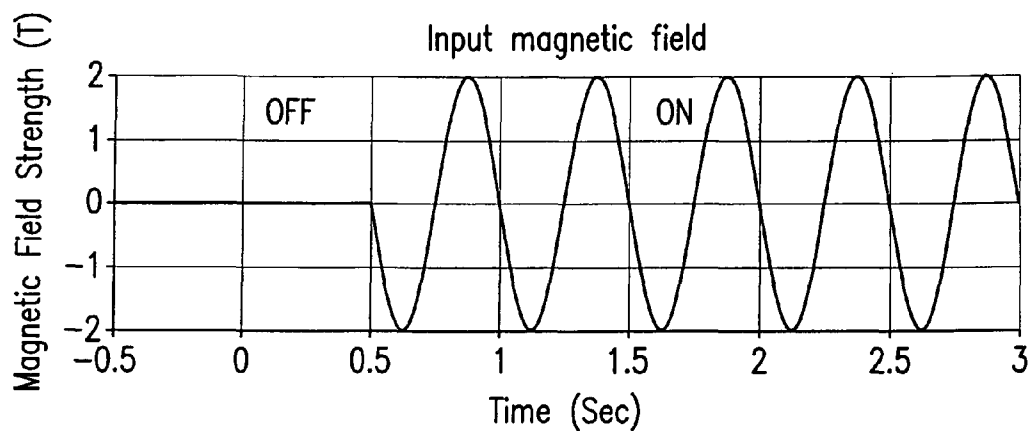


FIG. 11A

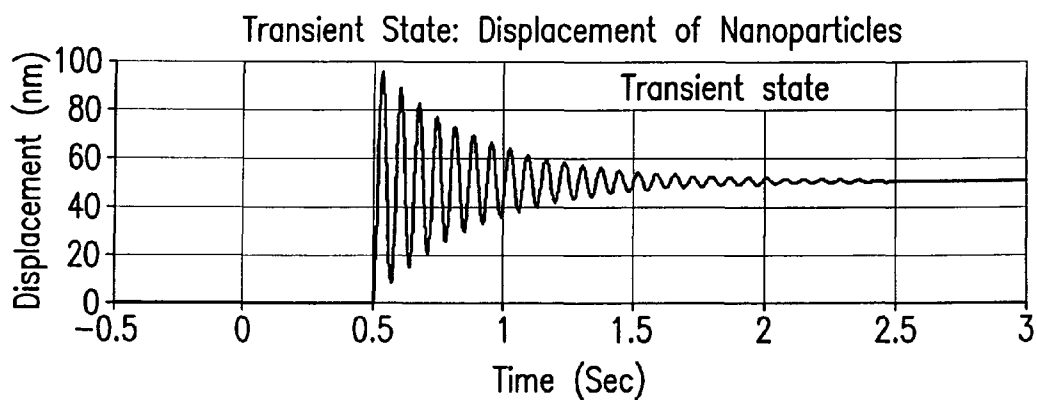


FIG. 11B

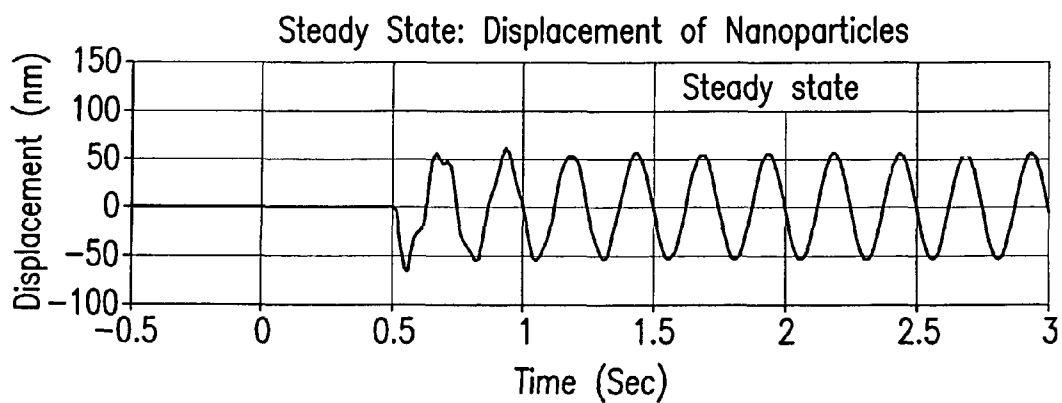


FIG. 11C

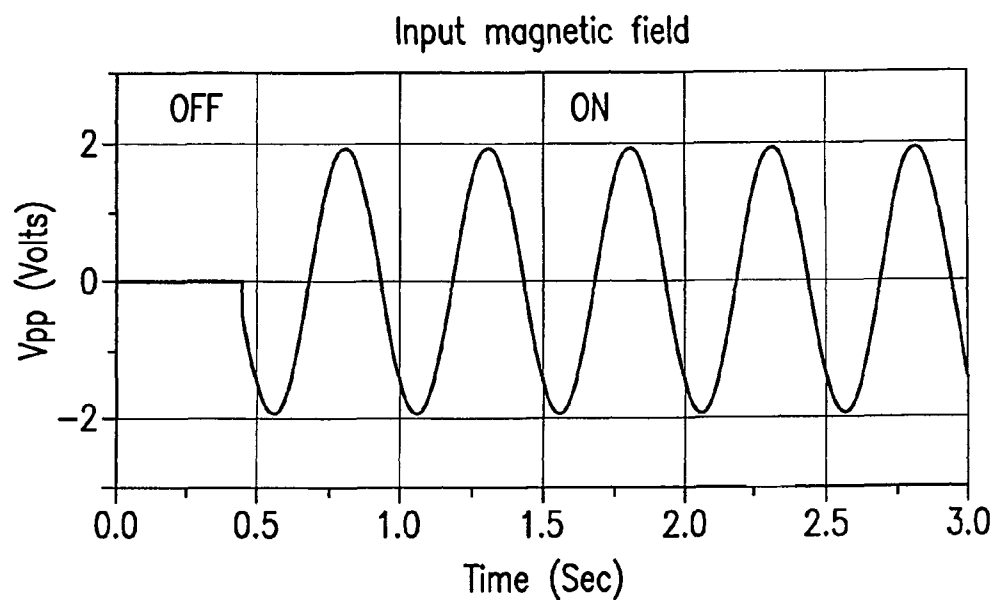


FIG.11D

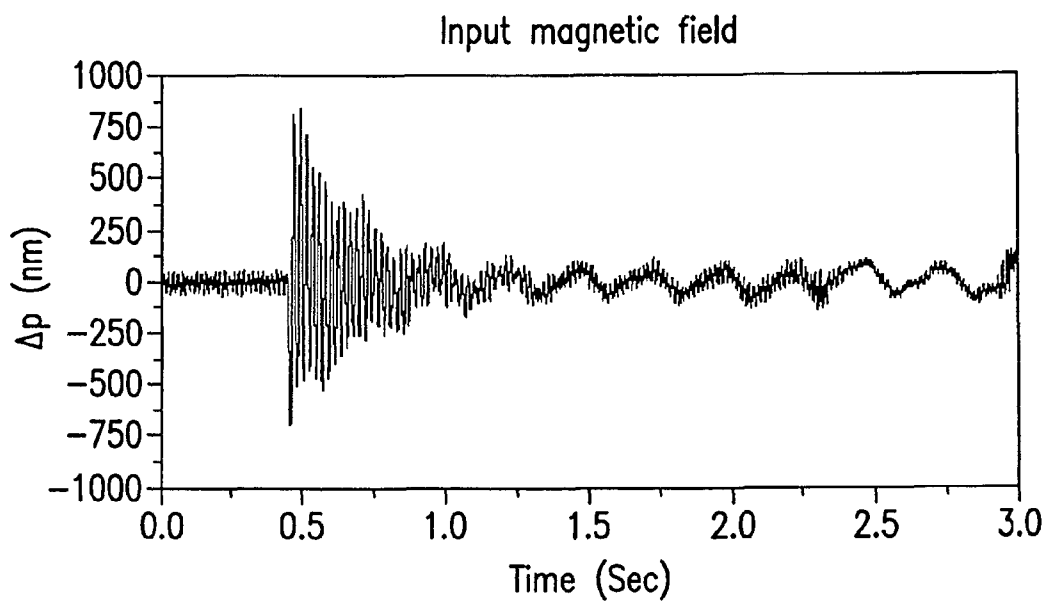


FIG.11E

1

OPTICAL COHERENCE TOMOGRAPHIC DETECTION OF CELLS AND COMPOSITIONS

CROSS-REFERENCE TO RELATED APPLICATIONS

This application claims priority to U.S. Provisional Application No. 60/685,559, filed on May 27, 2005. The aforementioned application is herein incorporated by reference in its entirety.

BACKGROUND

Arteriosclerosis, also known as atherosclerosis, is a common human ailment arising from the deposition of fatty-like substances, referred to as atheromas or plaques, on the walls of blood vessels. While some plaques are relatively stable, others are vulnerable to rupture and release their contents into the bloodstream, causing a blood clot to form. Heart attacks and other acute cardiovascular events usually result from the rupture of high-risk, vulnerable plaques in coronary arteries. Vulnerable plaques are believed to have three major characteristics—a deposit of lipids, a thin cap of fibrous material covering the lipid pool, and infiltration of the immune cells called macrophages. Such deposits occur in both the peripheral blood vessels and the coronary vessels. When deposits accumulate in localized regions of a blood vessel, stenosis, or narrowing of the vascular channel occurs. Blood flow is restricted and the person's health is at serious risk. Early detection and characterization of arterial plaque can identify patients who are unaware that they are at risk of suffering a myocardial infarction or other cardiovascular events such as stroke.

Optical coherence tomography (OCT) has been used to successfully image various organs and tissues. OCT can produce a relatively high resolution image, especially when compared to other imaging modalities. OCT imaging of arterial plaques, however, has had limited success and has been unsatisfactory for identification of vulnerable plaques. Methods and apparatuses for high resolution OCT images are needed for imaging arterial plaques and for identifying vulnerable plaques. Moreover, similar methods and apparatuses are needed for imaging of other normal and diseased tissues, compositions, cells, and pathologies in a subject, including cancer and pre-cancerous conditions.

SUMMARY

Provided herein are systems and methods for the detection of cells and compositions using optical coherence tomography.

The methods, systems, and apparatuses are set forth in part in the description which follows, and in part will be obvious from the description, or can be learned by practice of the methods, apparatuses, and systems. The advantages of the methods, apparatuses, and systems will be realized and attained by means of the elements and combinations particularly pointed out in the appended claims. It is to be understood that both the foregoing general description and the following detailed description are exemplary and explanatory only and are not restrictive of the methods, apparatuses, and systems, as claimed.

BRIEF DESCRIPTION OF THE DRAWINGS

The accompanying drawings, which are incorporated in and constitute a part of this specification, illustrate aspects of

2

the methods, apparatuses, and systems and together with the description, serve to explain the principles of the methods, apparatuses, and systems.

FIG. 1 is a block diagram illustrating an exemplary phase sensitive OCT system.

FIG. 2 is a block diagram illustrating an exemplary phase sensitive multi-channel OCT system.

FIG. 3 is a schematic diagram illustrating aspects of the exemplary phase sensitive OCT system of FIG. 1.

FIG. 4 is schematic diagram illustrating aspects of the exemplary phase sensitive multi-channel OCT system of FIG. 2.

FIGS. 5A and B show solenoid drive signal and optical pathlength change observed in a mouse imaged with metallic nanoparticles (A) and a mouse imaged without metallic nanoparticles (B).

FIG. 6 shows a schematic diagram of a differential phase optical coherence tomography (DP-OCT) system combined with a magnetic field generator: (a) DP-OCT system, (b) collinear configurations of the DP-OCT sample path and design of the magnetic field generator containing a conical iron core.

FIG. 7 shows the optical path length change (Δp) in livers with different SPIO doses (1.0, 0.1 mmol Fe/kg and saline control) using focused magnetic field excitation (2 Hz, 4 V_{pp}) (a). Optical path length change (Δp) in specimens with doses 1.0 mmol Fe/kg SPIO (b), 0.1 mmol Fe/kg SPIO, and a saline control liver. The applied magnetic flux density strength is B_z=0.47 Tesla at the liver specimen.

FIG. 8 shows the maximum optical path length change (Δp) in iron-laden liver specimens due to nanoparticle movement in response to a focused magnetic field for mice injected with various SPIO doses (1.0 and 0.1 mmol Fe/kg). The input frequency is 2 Hz with applied voltage ranging from 2 to 8 V_{pp} (a) and magnetic field strength at each input voltage (b).

FIG. 9 shows the Optical path length change (Δp) in iron-laden liver specimens due to nanoparticle movement in response to a focused magnetic field with a swept frequency (1~10 Hz) input for mice injected with various SPIO doses (1.0 and 0.1 mmol Fe/kg). (a). Optical path length change (Δp) at 1.0 mmol Fe/kg SPIO dose (b), 0.1 mmol Fe/kg SPIO dose (c), and a saline control liver (d). The applied focused magnetic flux density is 1.3 Tesla at the specimen.

FIG. 10 shows the maximum optical path length change (Δp) in iron-laden liver specimens due to nanoparticle movement in response to a focused magnetic field with a swept frequency (1~10 Hz) input for mice injected with various SPIO doses (1.0 and 0.1 mmol Fe/kg). Input swept frequency ranged from 1~10 Hz over 2 seconds with input voltages increasing from 2 to 10 V_{pp} (a) and magnetic field strength at each input voltage (b).

FIG. 11 shows optical path length change (Δp) in iron-laden rabbit arteries (0.1 Fe/kg) measured in response to 2 Hz frequency sinusoidal input.

DETAILED DESCRIPTION

The methods, apparatuses, and systems can be understood more readily by reference to the following detailed description of the methods, apparatuses, and systems and the Examples included therein and to the Figures and their previous and following description.

Before the present compounds, compositions, articles, devices, and/or methods are disclosed and described, it is to be understood that these are not limited to specific synthetic methods, specific components, or to particular compositions, as such may, of course, vary. It is also to be understood that the

terminology used herein is for the purpose of describing particular embodiments only and is not intended to be limiting.

As used in the specification and the appended claims, the singular forms “a,” “an” and “the” include plural referents unless the context clearly dictates otherwise. Thus, for example, reference to “a nanoparticle” includes mixtures of nanoparticles, reference to “a nanoparticle” includes mixtures of two or more such nanoparticles, and the like.

Ranges may be expressed herein as from “about” one particular value, and/or to “about” another particular value. When such a range is expressed, another embodiment includes from the one particular value and/or to the other particular value. Similarly, when values are expressed as approximations, by use of the antecedent “about,” it will be understood that the particular value forms another embodiment. It will be further understood that the endpoints of each of the ranges are significant both in relation to the other endpoint, and independently of the other endpoint.

“Optional” or “optionally” means that the subsequently described event or circumstance may or may not occur, and that the description includes instances where said event or circumstance occurs and instances where it does not. For example, the phrase “optionally substituted shelled metals” means that shelled metals may or may not be substituted and that the description includes both unsubstituted shelled metals and shelled metals where there is substitution.

As used throughout, by a “subject” is meant an individual. Thus, the “subject” can include domesticated animals, such as cats, dogs, etc., livestock (e.g., cattle, horses, pigs, sheep, goats, etc.), laboratory animals (e.g., mouse, rabbit, rat, guinea pig, etc.) and birds. In one aspect, the subject is a mammal such as a primate or a human. The term does not denote a particular age or sex. Thus, adult and newborn subjects, as well as fetuses, whether male or female, are intended to be covered.

Reference will now be made in detail to exemplary aspects of the systems, methods, apparatuses, and/or compositions, examples of which are illustrated in the accompanying drawings.

Provided herein are methods, compositions and apparatuses for detecting a cell and/or a metallic composition using optical coherence tomography (OCT). By a “cell” is meant one or more cell of, or derived from, a living organism or subject. The cell or cells can be located within a subject or can be located ex vivo. The disclosed methods, compositions and apparatuses for detecting a cell and/or a metallic composition are described herein variously by reference to cell(s), composition(s) and/or metallic composition(s). It will be understood that description of various aspects of the disclosed methods, compositions and apparatuses by reference to one or a subset of cell(s), composition(s) or metallic composition(s) constitutes description of that aspect of the disclosed methods, compositions and apparatuses to the non-referenced cell(s), composition(s) and metallic composition(s), unless the context clearly indicates otherwise.

An exemplary method for detecting a cell comprises applying a magnetic field to the cell. A cell can comprise a cellular membrane and a metallic composition. Optionally, the metallic composition is a metallic nanoparticle that was administered to the subject or otherwise brought into contact with the cell.

The metallic composition can be located within the cell, including in the cell’s cellular membrane, or on the outside of the cell. If the metallic particle is located on the outside of the cell, it can be connected or targeted to the exterior surface of

the cell’s cellular membrane. Exemplary methods of targeting or connecting a metallic composition to a cell are described herein.

The applied magnetic field can interact with the metallic composition whether it is located within the cell or located external and connected to the cell. The interaction of the magnetic field with the composition can cause a change in the cell. A change “in” the cell is not limited to changes internal to the cell’s cellular membrane. A change “in” the cell is inclusive of changes within the cell, and also includes any change to, of, or in the cell caused by the interaction of the magnetic field with the composition. For example, changes that can occur “in” the cell include movement of the cell, movement of the metallic composition, a change in the cellular membrane tension level of the cell, and a change in the internal strain field of the cell. Changes in the cell that cause changes, including those listed above, of neighboring or surrounding cells or tissues can also be detected. Thus, changes in a cell can cause changes in surrounding cells or tissues. The changes in the surrounding cells or tissues can be detected using the methods and systems described herein. Compositions located within or external to the cell can cause one or more detectable changes in the cell when contacted by an applied magnetic field.

A detectable internal strain field is generated in a cell when a metallic composition, including a metallic nanoparticle, is under the action of an external force. The external force may be provided by the application of an external magnetic flux density (B). Action of the external force on each metallic composition can produce movement of the metallic composition ($z_{np}(t)$) that produces a change in the cellular membrane tension level or an internal strain field within a cell. Action of a force on each metallic composition in a cell or tissues produces a movement of the metallic composition ($z_{np}(t)$). Movement of the metallic composition can be along the z-direction. The metallic composition can also have movement in any direction that can be written as vector displacement, $u_{np}(r_o)$ for a metallic composition positioned at r_o . Metallic composition displacement $u_{np}(r_o)$ can produce a displacement field ($u(r, r_o)$) in the proteins in the cell containing the metallic composition and surrounding cells. In the case of a homogeneous elastic media, the displacement field ($u(r, r_o)$) can be computed for a semi-infinite half-space following, for example, the method of Mindlin (R. D. Mindlin, A force at a point of a semi-infinite solid, Physics 1936, 7:195-202, which is incorporated by reference for the methods taught therein). In the case of an inhomogeneous viscoelastic media, a finite element method numerical approach can be applied to compute the displacement field in the cell. The displacement field ($u(r, r_o)$) produced by a metallic composition positioned at r_o can induce an internal strain field that is determined by change in the displacement field along a particular direction. The strain field ($\epsilon_{ij}(r, r_o)$) is a tensor quantity and is given by,

$$\epsilon_{ij}(r, r_o) = \frac{\partial u_i(r, r_o)}{\partial x_j}$$

where $u_i(r, r_o)$ is the i’th component of the displacement field and x_j is the jth coordinate direction. For example, when j=3, x_3 is the z-direction. The internal strain field in a cell due to all metallic compositions in the cell and surrounding cells is a superposition of the strain fields due to each metallic composition.

The change in the cell can be detected using optical coherence tomographic imaging modalities. Thus, the cell can be

detected by detecting the change in the cell caused by the interaction of the magnetic field with the metallic composition using such a modality. The change can be detected using a phase sensitive optical coherence tomographic imaging modality. Non-limiting examples of phase sensitive optical coherence tomographic (OCT) imaging modalities are described herein. Phase sensitive OCT imaging modalities can comprise a probe for transmitting and receiving light energy to and from the cell. The probe can be sized, shaped and otherwise configured for intravascular operation. The probe can further comprise a magnetic source for applying the magnetic field to the cell. The magnetic field can be applied to the cell from a magnetic source located external to the subject or internal to the subject. The external source can be located in a probe or can be distinct from a probe.

The metallic composition can comprise a plurality of metallic nanoparticles. The nanoparticles can be substantially spherical in shape and can have a diameter from about 0.1 nanometers (nm) to about 1000.0 nm. The nanoparticles are not, however, limited to being spherical in shape. Thus, the nanoparticles are asymmetrical in shape. If the nanoparticles are asymmetrical in shape, the largest cross sectional dimension of the nanoparticles can be from about 0.1 nanometers (nm) to about 1000.0 nm in length.

The metallic composition can comprise metal having non-zero magnetic susceptibility or zero magnetic susceptibility or combinations of non-zero and zero magnetic susceptibility metals. Thus, if the composition comprises nanoparticles, the nanoparticles can all have a non-zero magnetic susceptibility or a zero magnetic susceptibility or a combination of particles having a non-zero magnetic susceptibility and a zero magnetic susceptibility. Metallic compositions having a non-zero magnetic susceptibility can comprise a material selected from the group consisting of iron oxide, iron, cobalt, nickel, chromium and combinations thereof. The metallic compositions can comprise metal having non-zero electrical conductivity or zero electrical conductivity or combinations of non-zero and zero electrical conductivity metals. Also provided is a method for detecting a composition, the method wherein the composition comprises a magnetic or paramagnetic material. Any magnetic or paramagnetic material, whether metallic or non-metallic, can be used in the described methods or with the described systems. In this regard, any material can be used that can cause a change in a cell or can be detected using phase sensitive optical coherence tomography when contacted with an applied magnetic field. Similarly, non-metallic, not magnetic particles can be used to cause a change in a cell or can be detected using phase sensitive optical coherence tomography when contacted with an applied magnetic field using the methods and systems described herein.

The systems, apparatuses and methods can be practiced using metallic compositions without magnetic susceptibility. When using metallic compositions without magnetic susceptibility, or when using compounds having a non-zero magnetic susceptibility, an electrical eddy current can be induced in the composition.

To induce an eddy current in a metallic composition a first time-varying magnetic field can be applied to a cell. The first magnetic field can interact with a metallic composition within or external to the cell to induce an electrical eddy current within the metallic composition. A second magnetic field can be applied to the cell that interacts with the induced eddy current to cause a change in the cell. The cell can be detected by detecting the change in the cell caused by the interaction of the second magnetic field with eddy current using a phase sensitive optical coherence tomographic imaging modality. Exemplary changes in the cell caused by the interaction of the

second magnetic field with the eddy current include movement of the cell, movement of the metallic composition, a change in the cellular membrane tension level, and a change in the internal strain field of the cell.

Thus, a metallic composition or a nanoparticle that does not have a significant magnetic permeability can be used. For example, although gold nanoparticles do not have significant magnetic permeability many target-specific molecular agents (e.g., antibodies) can be conjugated to the nanoparticle surface. When using a high-conductivity particle for detection, a magnetic dipole can be induced in the particle by exposing to a time-varying magnetic field ($B(t)$).

The time-varying magnetic field ($B(t)$) can cause an electromotive force or potential in the particle that can induce a volumetric and surface electric eddy-current in the high-conductivity nanoparticle. Exemplary circuitry for a magnetic pulser that can be used to produce an eddy current is described in G H Schroder, Fast pulsed magnet systems, Handbook of Accelerator Physics and Engineering, A. Chao and M. Tinger, Eds. 1998 or in IEEE transactions on instrumentation and measurement, VOL. 54, NO. 6, December 2005, pp 2481-2485, which are incorporated herein by reference for the circuitry and methods described therein.

The eddy-current can produce time-varying magnetic moment that can interact with a second applied magnetic field (B_2). The induced eddy-current in the high-conductivity nanoparticle or metallic composition and the second applied magnetic field can interact to produce a torque or twist on the nanoparticle or metallic composition. The induced torque can twist the nanoparticle that is mechanically linked to a target in the cell (e.g., the membrane) or located inside the cell. The twisting motion of the nanoparticle can modify the internal strain field of the cell (surrounding cells and tissue) which can be detected using phase sensitive optical coherence tomography.

In exemplary embodiments, large magnetic fields can be generated by low temperature superconducting magnets. These magnets need only be "charged" once, maintained at a low temperature and do not require an external current to maintain the magnetic field.

A metallic composition can be administered to the subject. Administration of exogenous metallic compositions, for example, metallic nanoparticles is described in greater detail below. Optionally, the cell can be located within a subject and the metallic composition can be administered to the subject. Optionally, the cell can be a macrophage and at least one metallic nanoparticle can be located within the macrophage or can be connected to the macrophage. The macrophage can be located in an atherosclerotic plaque within the subject. The macrophage can also be located within the eye of the subject.

The change in the cell caused by the interaction of the magnetic field with the metallic composition can be detected by generating a phase sensitive optical coherence tomographic image. A phase sensitive optical coherence tomographic image can comprise one or more lines of phase sensitive light energy data captured using a phase sensitive optical coherence tomography modality, wherein at least one line is captured during the application of the magnetic field.

One or more data line can be produced by generating light energy and transmitting at least a first portion of the generated light energy onto a reference reflector wherein at least a portion of the transmitted first portion of light energy is reflected by the reference reflector. At least a second portion of the generated light energy can be transmitted to contact the cell wherein at least a portion of the light energy that contacts the cell is reflected by the cell. The light energy reflected by the reference reflector and by the cell can be received, and the

received light energy can be combined, and the received light energy can interfere. The combined light energy is processed to produce a phase sensitive optical coherence data line.

One or more data lines can also be produced by generating light energy and transmitting at least a first portion of the generated light energy onto a reference reflector wherein at least a portion of the transmitted first portion of light energy is reflected by the reference reflector. At least a second portion of the generated light energy can be transmitted to contact the metallic composition wherein at least a portion of the light energy that contacts the metallic composition is reflected by the composition. The light energy reflected by the reference reflector and by the composition can be received. The received light energy can be combined, wherein the received light energy interferes. The combined light energy can be processed to produce the phase sensitive optical coherence data line.

Phase sensitive light energy data lines can include the spectral dependent complex amplitude of light reflected from the cell, $A_c(v)$, where v is the optical frequency of light. More precisely, what can be measured is product of the amplitudes of light reflected from the cell and reference: $A_c(v) \cdot A_r(v)^*$ where $A_r(v)^*$ is the conjugate of the spectrally-dependent complex amplitude of light reflected from the reference. The quantity $A_c(v) \cdot A_r(v)^*$ can be used to determine $A_c(\tau)$ the phase sensitive amplitude of light backreflected from the cell/tissue at different time-delays τ by using a time-frequency transformation (e.g., Fourier).

A plurality of phase sensitive light energy data lines can be captured and used to construct an image. A phase sensitive image produced using the described systems and methods can have a phase sensitive resolution of at least about 30.0 nanometers (nm), 25.0 nm, 15.0 nm, 10.0 nm, 5.0 nm, 4.0 nm, 3.0 nm, or 2.0 nm. A plurality of phase sensitive light energy data lines can be spatially and temporally distinct and the image can comprise a B-mode image frame of at least two of the data lines. The plurality of phase sensitive light energy data lines can also be temporally distinct and the image can comprise an M-mode image comprising at least two of the lines.

When a plurality of lines are used to create an image, at least a first phase sensitive light energy data line can be captured prior to the application of the magnetic field and at least a second phase sensitive light energy data line can be captured during application of the magnetic field. The magnetic field strength can be altered between the capture of data lines or between the capture of images. For example, at least a first phase sensitive light energy data line can be captured during the application of the magnetic field, wherein the magnetic field has a first predetermined strength and at least a second phase sensitive light energy data line during application of a second magnetic field having a second predetermined strength. The captured lines can be processed to create an image. Optionally, the first predetermined strength can be less than the second predetermined strength.

The described methods allows for the construction of both conventional intensity based OCT B-scan images and phase sensitive B-scan images. The phase sensitive B-scan images for viewing can correspond to changes in phase formed by at least two phase sensitive B-scan images corresponding to different magnetic field strengths (one of which can be zero magnetic field strength). At least two types of images can be viewed—one, a conventional intensity based OCT B-scan image and second a phase sensitive B-scan image formed by the difference of two phase sensitive images recorded at different magnetic field strengths.

Also provided are methods for detecting a composition comprising metal by applying a magnetic field to the compo-

sition, wherein the magnetic field interacts with the composition. The metallic composition can be detected using a phase sensitive optical coherence tomographic imaging modality. As described throughout, the composition can be located in a cell or can be connected to a cell. The composition can also be located in connection with non-cellular biological matter. For example, non-cellular biological matter can include a protein, a lipid, a peptide, and a nucleic acid.

The methods of detecting cells and compositions using optical coherence tomography can comprise administering a plurality of metallic nanoparticles to a subject.

Optionally, at least one administered nanoparticle localizes within a macrophage located in the subject. At least one administered nanoparticle can also be optionally configured to localize to a target site in the subject.

In the methods described herein, a nanoparticle comprising a material with non-zero magnetic susceptibility can be positionally moved in vivo or in vitro by an applied magnetic field. A material of non-zero magnetic susceptibility can include a variety of materials. For example, the nanoparticle can comprise any physiologically tolerable magnetic material or combinations thereof. The term magnetic material can optionally include any material displaying ferromagnetic, paramagnetic or superparamagnetic properties. For example, the nanoparticles can comprise a material selected from the group consisting of iron oxide, iron, cobalt, nickel, and chromium. Metallic compositions as described throughout, including administered nanoparticles, can be magnetic. Optionally, a nanoparticle comprises iron oxide. When a nanoparticle comprises metal or magnetic materials, it can be moved while in the subject using an internally or externally applied magnetic field, as described below. Any relevant metal with non-zero magnetic susceptibility or combinations thereof can be used. Many useable metals are known in the art; however, any metal displaying the desired characteristics can be used. Nanoparticles can also comprise a combination of a material with a non-zero magnetic susceptibility and a material with a lower or zero magnetic susceptibility. For example, gold can be combined with higher magnetic susceptibility materials (e.g., iron). For example, gold coated iron can be used. Nanoparticles can also comprise polymers or other coating materials alone or in combination. Such polymers or coating materials can be used to attach targeting ligands, including but not limited to antibodies, as described below. When used in vivo, an administered nanoparticle can be physiologically tolerated by the subject, which can be readily determined by one skilled in the art.

Nanoparticles can be solid, hollow or partially hollow and can be spherical or asymmetrical in shape. Optionally, the cross section of an asymmetric nanoparticle is oval or elliptical. As one of skill in the art will appreciate, however, other asymmetric shapes can be used. The nanoparticles can comprise shelled or multi-shelled nanoparticles. Shelled or multi-shelled nanoparticles can have targeting ligands conjugated to the shell material wherein the targeting ligand has an affinity for or binds to a target site in a subject or ex vivo. Such shelled or multi-shelled nanoparticles can be made, for example, using techniques known in the art, for example, as described in Loo et al., "Nanoshell-Enabled Photonics-Based Imaging and Therapy of Cancer," *Tech. Cancer Res. and Treatment*, (2004) 3(1) 33-40, which is incorporated herein by reference for the methods taught herein. Further, Oldenburg et al., "Nanoengineering of Optical Resonances," *Chemical Physics Letters* (1998) 288, 243-247, is incorporated herein for methods of nanoshell synthesis.

A metallic composition, including a nanoparticle, can be configured to localize to a target site within the subject. For

example, the metallic composition can be configured to localize to a neoplastic cell, to a peptide, to a protein, or to a nucleic acid. Optionally, the target site is an extracellular domain of a protein. A variety of cell types can also be targets of the metallic compositions. For example, target cells can be selected from one or more of a neoplastic cell, a squameous cell, a transitional cell, a basal cell, a muscle cell, an epithelial cell, and a mucosal cell. The target cells can also be located at different anatomical locations within a subject. For example, the cell can be located in the subject at an anatomical location selected from the group consisting of a lung, bronchus, intestine, stomach, colon, eye, heart, blood vessel, cervix, bladder, urethra, skin, muscle, liver, kidney, and blood.

One or more administered nanoparticle can localize to a desired target within the subject using passive or active targeting mechanisms. Passive targeting mechanisms take advantage of the subject's inherent defense mechanisms to highlight phagocytic cells naturally responsible for particle clearance. For example, macrophage rich areas are a pathological correlate to an unstable atherosclerotic plaque in a subject. Moreover, administered nanoparticles, for example, small superparamagnetic and ultrasmall superparamagnetic particles of iron oxide, are avidly taken up, or engulfed by, macrophages located in unstable plaques. Thus, through the subject's natural defense mechanism, wherein macrophages accumulate in an unstable atherosclerotic plaque and engulf administered nanoparticles, administered nanoparticles can passively target the unstable plaque. Similarly, macrophages located in the eye of a subject can engulf nanoparticles. Such passive targeting of nanoparticles can be used with the methods and apparatuses described herein to highlight a plaque's instability or to highlight other accumulation of phagocytic cells.

Active targeting mechanisms can refer to the use of ligand-directed, site-specific targeting of nanoparticles. A nanoparticle can be configured to localize to a desired target site in a subject using a wide variety of targeting ligands including, but not limited to, antibodies, polypeptides, peptides, nucleic acids, and polysaccharides. Such nanoparticles are referred to herein as "targeted nanoparticles." Targeting ligands or fragments thereof can be used to target a nanoparticle to cellular, or other endogenous or exogenous biomarkers in the subject. Such a biomarkers or "target sites" can include, but are not limited to, proteins, polypeptides, peptides, polysaccharides, lipids, or antigenic portions thereof, which are expressed within the subject. When active targeting mechanisms are used to target a cell, the targeted nanoparticle can be optionally internalized by the targeted cell.

Thus, using the disclosed methods, at least one administered nanoparticle can optionally localize within a macrophage located in the subject and/or at least one administered targeted nanoparticle can localize to a desired target site in the subject.

The methods and apparatuses are not, however, limited to in vivo administration to a subject. As would be clear to one skilled in the art, nanoparticles, including targeted nanoparticles, can be administered in vitro to an ex vivo sample with localization of the nanoparticle to a desired target site and subsequent imaging occurring in vitro. Moreover, a composition, including at least one nanoparticle can be administered to a subject in vivo, and a sample can be subsequently taken from the subject and imaged ex vivo using the methods, systems, and apparatuses described herein.

When using a targeted nanoparticle the target site in vivo or in vitro can be endogenous or exogenous. The target site can be selected from the group consisting of an organ, cell, cell type, blood vessel, thrombus, fibrin and infective agent anti-

gens or portions thereof. Optionally, the target site can be a neoplastic cell. The target site can also be an extracellular domain of a protein. Furthermore, the target site can be selected from the group consisting of a lung, bronchus, intestine, stomach, colon, heart, brain, blood vessel, cervix, bladder, urethra, skin, muscle, liver, kidney and blood. The target site can also be a cell. For example, a cell can be selected from the group consisting of, but not limited to, a neoplastic cell, a squameous cell, a transitional cell, a basal cell, a muscle cell, an epithelial cell, a lymphocyte, a leukocyte, an monocyte, a red blood cell, and a mucosal cell.

Thus, targeted nanoparticles can be targeted to a variety of cells, cell types, antigens (endogenous and exogenous), epitopes, cellular membrane proteins, organs, markers, tumor markers, angiogenesis markers, blood vessels, thrombus, fibrin, and infective agents. For example, targeted nanoparticles can be produced that localize to targets expressed in a subject. Optionally, the target can be a protein, and can be a protein with an extracellular or transmembrane domain. Optionally, the target can be the extracellular domain of a protein.

Desired targets can be based on, but not limited to, the molecular signature of various pathologies, organs and/or cells. For example, adhesion molecules such as integrin $\alpha v \beta 3$, intercellular adhesion molecule-1 (I-CAM-1), fibrinogen receptor GPIIb/IIIa and VEGF receptors are expressed in regions of angiogenesis, inflammation or thrombus. These molecular signatures can be used to localize nanoparticles through the use of a targeting ligand. The methods described herein optionally use nanoparticles targeted to one or more of VEGFR2, I-CAM-1, $\alpha v \beta 3$ integrin, αv integrin, fibrinogen receptor GPIIb/IIIa, P-selectin, and/or mucosal vascular addressin cell adhesion molecule-1.

As used in this invention, the term "epitope" is meant to include any determinant capable of specific interaction with a targeting ligand as described below. Epitopic determinants can consist of chemically active surface groupings of molecules such as amino acids or sugar side chains and can have specific three dimensional structural characteristics, as well as specific charge characteristics.

Targeting ligands specific for a molecule that is expressed or over-expressed in a cell, tissue, or organ targeted for imaging, such as pre-cancerous, cancerous, neoplastic, or hyperproliferative cells, tissues, or organs, can be used with the nanoparticles described herein. This use can include the in vivo or in vitro imaging, detection, or diagnosis of pre-cancerous, cancerous, neoplastic or hyperproliferative cells in a tissue or organ. The compositions and methods of the invention can be used or provided in diagnostic kits for use in detecting and diagnosing cancer.

As used herein, a targeted cancer to be imaged, detected or diagnosed can be selected from, but are not limited to, the group comprising lymphomas (Hodgkins and non-Hodgkins), B cell lymphoma, T cell lymphoma, myeloid leukemia, leukemias, mycosis fungoides, carcinomas, carcinomas of solid tissues, squamous cell carcinomas, adenocarcinomas, sarcomas, gliomas, blastomas, neuroblastomas, plasmacytomas, histiocytomas, melanomas, adenomas, hypoxic tumors, myelomas, AIDS-related lymphomas or sarcomas, metastatic cancers, bladder cancer, brain cancer, nervous system cancer, squamous cell carcinoma of head and neck, neuroblastoma/glioblastoma, ovarian cancer, skin cancer, liver cancer, melanoma, squamous cell carcinomas of the mouth, throat, larynx, and lung, colon cancer, cervical cancer, cervical carcinoma, breast cancer, epithelial cancer, renal cancer, genitourinary cancer, pulmonary cancer, esophageal

carcinoma, head and neck carcinoma, hematopoietic cancers, testicular cancer, colo-rectal cancers, prostatic cancer, or pancreatic cancer.

Pre-cancerous conditions to be imaged, detected or diagnosed include, but are not limited to, cervical and anal dysplasias, other dysplasias, severe dysplasias, hyperplasias, atypical hyperplasias, and neoplasias. As would be clear to one skilled in the art, however, additional cancers and pre-cancerous conditions can be imaged, detected or diagnosed using the methods and apparatuses described herein.

Using methods known in the art, and as described herein, targeting ligands, such as polyclonal or monoclonal antibodies, can be produced to desired target sites in a subject. Thus, a targeted nanoparticle can further comprise an antibody or a fragment thereof. Methods for preparing and characterizing antibodies are well known in the art (See, e.g., *Antibodies: A Laboratory Manual*, Cold Spring Harbor Laboratory, 1988; incorporated herein by reference for the methods taught therein).

Monoclonal antibodies can be obtained from a population of substantially homogeneous antibodies, i.e., the individual antibodies comprising the population are identical except for possible naturally-occurring mutations that can be present in minor amounts. Thus, the modifier "monoclonal" indicates the character of the antibody as not being a mixture of discrete antibodies.

For example, the monoclonal antibodies of the invention can be made Using the hybridoma method first described by Kohler & Milstein, *Nature* 256:495 (1975), or can be made by recombinant DNA methods (Cabilly, et al., U.S. Pat. No. 4,816,567).

In the hybridoma method, a mouse or other appropriate host animal, such as hamster can be immunized to elicit lymphocytes that produce or are capable of producing antibodies that will specifically bind to the antigen used for immunization. Alternatively, lymphocytes can be immunized in vitro. Lymphocytes can be then fused with myeloma cells using a suitable fusing agent, such as polyethylene glycol, to form a hybridoma cell (Goding, *Monoclonal Antibodies: Principles and Practice*, pp.59-103 (Academic Press, 1986)).

DNA encoding a monoclonal antibody can be readily isolated and sequenced using conventional procedures (e.g., by using oligonucleotide probes that are capable of binding specifically to genes encoding the heavy and light chains of murine antibodies). The hybridoma cells can serve as a preferred source of such DNA. Once isolated, the DNA can be placed into expression vectors, which can then be transfected into host cells such as simian COS cells, Chinese hamster ovary (CHO) cells, or myeloma cells that do not otherwise produce immunoglobulin protein, to obtain the synthesis of monoclonal antibodies in the recombinant host cells. The DNA also can be modified, for example, by substituting the coding sequence for human heavy and light chain constant domains in place of the homologous murine sequences, Morrison, et al., *Proc. Nat. Acad. Sci* 81, 6851 (1984), or by covalently joining to the immunoglobulin coding sequence all or part of the coding sequence for a non-immunoglobulin polypeptide. In that manner, "chimeric" or "hybrid" antibodies can be prepared that have the binding specificity of an anti-cancer, pre-cancer, or hyperproliferative cell or other target molecule. Optionally, the antibody used herein is "humanized" or fully human.

Non-immunoglobulin polypeptides can be substituted for the constant domains of an antibody of the invention, or they can be substituted for the variable domains of one antigen-combining site of an antibody of the invention to create a chimeric bivalent antibody comprising one antigen-combin-

ing site having specificity for a first antigen and another antigen-combining site having specificity for a different antigen.

Chimeric or hybrid antibodies also can be prepared in vitro using known methods in synthetic protein chemistry, including those involving crosslinking agents.

Methods for humanizing non-human antibodies are well known in the art. Generally, a humanized antibody has one or more amino acid residues introduced into it from a source which is non-human. These non-human amino acid residues are often referred to as "import" residues, which are typically taken from an "import" variable domain. Humanization can be essentially performed following the method of Winter and co-workers (Jones et al., *Nature* 321, 522-525 (1986); Riechmann et al., *Nature* 332, 323-327 (1988); Verhoeyen et al., *Science* 239, 1534-1536 (1988)), by substituting rodent CDRs or CDR sequences for the corresponding sequences of a human antibody. Accordingly, such "humanized" antibodies are chimeric antibodies, wherein substantially less than an intact human variable domain has been substituted by the corresponding sequence from a non-human species. In practice, humanized antibodies are typically human antibodies in which some CDR residues and possibly some FR residues are substituted by residues from analogous sites in rodent antibodies.

Antibodies can be humanized with retention of high affinity for the target site antigen and other favorable biological properties. Humanized antibodies can be prepared by a process of analysis of the parental sequences and various conceptual humanized products using three dimensional models of the parental and humanized sequences. Three dimensional immunoglobulin models are commonly available and are familiar to those skilled in the art. Computer programs are available which illustrate and display probable three-dimensional conformational structures of selected candidate immunoglobulin sequences. Inspection of these displays permits analysis of the likely role of the residues in the functioning of the candidate immunoglobulin sequence, i.e. the analysis of residues that influence the ability of the candidate immunoglobulin to bind its antigen. In this way, FR residues can be selected and combined from the consensus and import sequence so that the desired antibody characteristic, such as increased affinity for the target site antigen(s), can be achieved. In general, the CDR residues are directly and most substantially involved in influencing antigen binding.

Human monoclonal antibodies can be made by a hybridoma method. Human myeloma and mouse-human heteromyeloma cell lines for the production of human monoclonal antibodies have been described, for example, by Kozbor, J. *Immunol.* 133, 3001 (1984), and Brodeur, et al., *Monoclonal Antibody Production Techniques and Applications*, pp. 51-63 (Marcel Dekker, Inc., New York, 1987).

Transgenic animals (e.g., mice) can be used that are capable, upon immunization, of producing a repertoire of human antibodies in the absence of endogenous immunoglobulin production. For example, it has been described that the homozygous deletion of the antibody heavy chain joining region (JH) gene in chimeric and germ-line mutant mice results in complete inhibition of endogenous antibody production. Transfer of the human germ-line immunoglobulin gene array in such germ-line mutant mice will result in the production of human antibodies upon antigen challenge. See, e.g. Jakobovits et al., *Proc. Natl. Acad. Sci. USA* 90, 2551-2555 (1993); Jakobovits et al., *Nature* 362, 255-258 (1993).

Alternatively, phage display technology (McCafferty et al., *Nature* 348, 552-553 (1990)) can be used to produce human antibodies and antibody fragments in vitro, from immunoglo-

bulin variable (V) domain gene repertoires from unimmunized donors. According to this technique, antibody V domain genes are cloned in-frame into either a major or minor coat protein gene of a filamentous bacteriophage, such as M13 or fd, and displayed as functional antibody fragments on the surface of the phage particle. Because the filamentous particle contains a single-stranded DNA copy of the phage genome, selections based on the functional properties of the antibody also result in selection of the gene encoding the antibody exhibiting those properties. Thus, the phage mimics some of the properties of the B-cell. Phage display can be performed in a variety of formats; for their review see, e.g. Johnson, Kevin S. and Chiswell, David J., *Current Opinion in Structural Biology* 3, 564-571 (1993). Several sources of V-gene segments can be used for phage display. Clackson et al., *Nature* 352, 624-628 (1991) isolated a diverse array of anti-oxazolone antibodies from a small random combinatorial library of V genes derived from the spleens of immunized mice. A repertoire of V genes from unimmunized human donors can be constructed and antibodies to a diverse array of antigens (including self-antigens) can be isolated essentially following the techniques described by Marks et al., *J. Mol. Biol.* 222, 581-597 (1991), or Griffith et al., *EMBO J.* 12, 725-734 (1993). In a natural immune response, antibody genes accumulate mutations at a high rate (somatic hypermutation). Some of the changes introduced can confer higher affinity, and B cells displaying high-affinity surface immunoglobulin are preferentially replicated and differentiated during subsequent antigen challenge. This natural process can be mimicked by employing the technique known as "chain shuffling" (Marks et al., *Bio/Technol.* 10, 779-783 (1992)). In this method, the affinity of "primary" human antibodies obtained by phage display can be improved by sequentially replacing the heavy and light chain V region genes with repertoires of naturally occurring variants (repertoires) of V domain genes obtained from unimmunized donors. This technique allows the production of antibodies and antibody fragments with affinities in the nM range. A strategy for making very large phage antibody repertoires (also known as "the mother-of-all libraries") has been described by Waterhouse et al., *Nucl. Acids Res.* 21, 2265-2266 (1993), and the isolation of a high affinity human antibody directly from such large phage library is reported by Griffith et al., *EMBO J.* (1994). Gene shuffling can also be used to derive human antibodies from rodent antibodies, where the human antibody has similar affinities and specificities to the starting rodent antibody. According to this method, which is also referred to as "epitope imprinting," the heavy or light chain V domain gene of rodent antibodies obtained by phage display technique is replaced with a repertoire of human V domain genes, creating rodent-human chimeras. Selection on antigen results in isolation of human variable capable of restoring a functional antigen-binding site, i.e. the epitope governs (imprints) the choice of partner.

When the process is repeated in order to replace the remaining rodent V domain, a human antibody is obtained (see PCT patent application WO 93/06213, published Apr. 1, 1993).

Unlike traditional humanization of rodent antibodies by CDR grafting, this technique provides completely human antibodies, which have no framework or CDR residues of rodent origin.

Bispecific antibodies are monoclonal, preferably human or humanized, antibodies that have binding specificities for at least two different antigens. One of the binding specificities is for a first antigen and the other one is for a second antigen.

Traditionally, the recombinant production of bispecific antibodies is based on the coexpression of two immunoglobulin heavy chain-light chain pairs, where the two heavy chains have different specificities (Millstein and Cuello, *Nature* 305, 537-539 (1983)).

Because of the random assortment of immunoglobulin heavy and light chains, these hybridomas (quadromas) produce a potential mixture of 10 different antibody molecules, of which only one has the correct bispecific structure. The purification of the correct molecule, which is usually done by affinity chromatography steps, is rather cumbersome, and the product yields are low. Similar procedures are disclosed in PCT application publication No. WO 93/08829 (published May 13, 1993), and in Traunecker et al., *EMBO* 10, 3655-3659 (1991). For further details of generating bispecific antibodies see, for example, Suresh et al., *Methods in Enzymology* 121, 210 (1986).

Heteroconjugate antibodies are also within the scope of the described compositions and methods. Heteroconjugate antibodies are composed of two covalently joined antibodies. Heteroconjugate antibodies can be made using any convenient cross-linking methods. Suitable cross-linking agents are well known in the art, and are disclosed in U.S. Pat. No. 4,676,980, along with a number of cross-linking techniques.

A variety of immunoassay formats can be used to select antibodies that selectively, bind with a desired target site or target site antigen. For example, solid-phase ELISA immunoassays are routinely used to select antibodies selectively immunoreactive with a protein, protein variant, or fragment thereof. See Harlow and Lane, *Antibodies, A Laboratory Manual*. Cold Spring Harbor Publications, New York, (1988), for a description of immunoassay formats and conditions that could be used to determine selective binding. The binding affinity of a monoclonal antibody can, for example, be determined by the Scatchard analysis of Munson et al., *Anal. Biochem.*, 107:220 (1980).

Not only can a targeted nanoparticle comprise an antibody or fragment thereof, but a targeted nanoparticle can also comprise targeting ligand that is a polypeptide or a fragment thereof. Optionally, polypeptides that are internalized by target cells can be attached to the surface of a nanoparticle. Ligands that are internalized can optionally be used for internalization of a nanoparticle into a target cell. A modified phage library can be used to screen for specific polypeptide sequences that are internalized by desired target cells. For example, using the methods described in Kelly et al., "Detection of Vascular Adhesion Molecule-1 Expression Using a Novel Multimodal Nanoparticle," *Circulation Res.*, (2005) 96:327-336, which is incorporated herein for the methods taught therein, polypeptides can be selected that are internalized by VCAM-1 expressing cells or other cells expressing a ligand of interest.

There are a number of methods for isolating proteins which can bind a desired target. For example, phage display libraries have been used to isolate numerous polypeptides that interact with a specific target. (See for example, U.S. Pat. Nos. 6,031,071; 5,824,520; 5,596,079; and 5,565,332 which are herein incorporated by reference at least for their material related to phage display and methods related to combinatorial chemistry). Thus targeted nanoparticles can comprise a polypeptide or fragments thereof that interact with a desired target. A targeted nanoparticle can also comprise a binding domain of an antibody or phage.

The term "polypeptide" or "peptide" is used broadly herein to mean two or more amino acids linked by a peptide bond. The term "fragment" or "proteolytic fragment" also is used herein to refer to a product that can be produced by a pro-

teolytic reaction on a polypeptide, i.e., a peptide produced upon cleavage of a peptide bond in the polypeptide. A fragment can be produced by a proteolytic reaction, but it should be recognized that a fragment need not necessarily be produced by a proteolytic reaction but can be produced using methods of chemical synthesis or methods of recombinant DNA technology, to produce a synthetic peptide that is equivalent to a proteolytic fragment. It should be recognized that the term "polypeptide" is not used herein to suggest a particular size or number of amino acids comprising the molecule, and that a polypeptide of the invention can contain up to several amino acid residues or more.

A nanoparticle can bind selectively or specifically to a desired target site, and/or can be internalized by a target cell. Such selective or specific binding and/or internalization can be readily determined using the methods, systems and apparatuses described herein. For example, selective or specific binding can be determined *in vivo* or *in vitro* by administering a targeted nanoparticle and detecting an increase in light scattering from the nanoparticle bound to a desired target site or internalized into the desired target cell. Detection of light scattering can be measured using the systems and apparatuses described below.

Thus, a targeted nanoparticle can be compared to a control nanoparticle having all the components of the targeted nanoparticle except the targeting characteristics, such as, for example, targeting ligand. By detecting phase sensitive image data from the targeted nanoparticle bound to a desired target site versus a control nanoparticle, the specificity or selectivity of binding or internalization can be determined. If an antibody, polypeptide, or fragment thereof, or other targeting ligand is used, selective or specific binding to a target can be determined based on standard antigen/polypeptide/epitope/antibody complementary binding relationships. Further, other controls can be used. For example, the specific or selective targeting of the nanoparticles can be determined by exposing targeted nanoparticles to a control tissue, which includes all the components of the test or subject tissue except for the desired target ligand or epitope. To compare a control sample to a test sample, levels of light scattering can be detected by, for example, the systems described below and the difference in levels or location can be compared.

A targeting ligand can be coupled to the surface or shell of at least one of the nanoparticle. Targeted nanoparticles comprising targeting ligands can be produced by methods known in the art. For example ligands, including but not limited to, antibodies, peptides, polypeptides, or fragments thereof can be conjugated to the nanoparticle surface.

Any method known in the art for conjugating a targeting ligand to a nanoparticle can be employed, including, for example, those methods described by Hunter, et al., *Nature* 144:945 (1962); David, et al., *Biochemistry* 13:1014 (1974); Pain, et al., *J. Immunol. Meth.* 40:219 (1981); and Nygren, J. *Histochem. and Cytochem.* 30:407 (1982). Established protocols have been developed for the labeling metallic nanoparticles with a broad range of biomolecules, including protein A, avidin, streptavidin, glucose oxidase, horseradish peroxidase, and IgG (antibodies). Nanoparticles can be prepared with bioorganic molecules on their surface (DNA, antibodies, avidin, phospholipids, etc). The nanoparticles can be characterized, modified, and conjugated with organic and biomolecules. Polymers or other intermediate molecules can be used to tether antibodies or other targeting ligands to the surface of nanoparticles. Methods of tethering ligands to nanoparticles are known in the art as described in, for example, Loo et al., "Nanoshell-Enabled Photonics-Based Imaging and Therapy

of Cancer, " *Tech. Cancer Res. and Treatment*, (2004) 3(1) 33-40, which is incorporated herein by reference for the methods taught herein.

Covalent binding of a targeting ligand to a nanoparticle can be achieved, for example, by direct condensation of existing side chains or by the incorporation of external bridging molecules. Many bivalent or polyvalent agents can be useful in coupling polypeptide molecules to other particles, nanoparticles, proteins, peptides or amine functions. Examples of coupling agents are carbodiimides, diisocyanates, glutaraldehyde, diazobenzenes, and hexamethylene diamines. This list is not intended to be exhaustive of the various coupling agents known in the art but, rather, is exemplary of the more common coupling agents that can be used.

Optionally, one can first derivatize an antibody if used, and then attach the nanoparticle to the derivatized product. As used herein, the term "derivatize" is used to describe the chemical modification of the antibody substrate with a suitable cross-linking agent. Examples of cross-linking agents for use in this manner include the disulfide-bond containing linkers SPDP (N-succinimidyl-3-(2-pyridyldithio)propionate) and SMPT (4-succinimidyl-oxy carbonyl- α -methyl- α -(2-pyridyldithio)toluene).

Targeting ligands can also be conjugated to nanoparticles using methods including the preparation of biotinylated antibody molecules and their consequent interaction with streptavidin/nanoparticle conjugates. This approach takes advantage of strong biospecific interaction between biotin and streptavidin and known protocols for immobilization of streptavidin on nanoparticles. Polypeptides with thiol terminated alkyl chains can be directly attached to the surface of nanoparticles using the procedures described in Elghanian, R., et al., *Selective colorimetric detection of polynucleotides based on the distance-dependent optical properties of gold nanoparticles*. *Science*, 1997. 277(5329): p. 1078-1080 (incorporated by reference for the methods taught therein). For conjugation procedure one can use a mixture of thiol terminated polypeptides and relatively small mercaptoacetic molecules to avoid high density immobilization of the polypeptides.

Targeted nanoparticles can be prepared with a biotinylated surface and an avidinated antibody, peptide, polypeptide or fragment thereof can be attached to the nanoparticle surface using avidin-biotin bridging chemistry. Avidinated nanoparticles can be used and a biotinylated antibody or fragment thereof or another biotinylated targeting ligand or fragments thereof can be administered to a subject. For example, a biotinylated targeting ligand such as an antibody, protein or other bioconjugate can be used. Thus, a biotinylated antibody, targeting ligand or molecule, or fragment thereof can bind to a desired target within a subject. Once bound to the desired target, the nanoparticle with an avidinated surface can bind to the biotinylated antibody, targeting molecule, or fragment thereof. When bound in this way, light energy can be transmitted to the bound nanoparticle, which can produce light scattering of the transmitted light. An avidinated nanoparticle can also be bound to a biotinylated antibody, targeting ligand or molecule, or fragment thereof prior to administration to the subject.

When using a targeted nanoparticle with a biotinylated surface or an avidinated surface a targeting ligand can be administered to the subject. For example, a biotinylated targeting ligand such as an antibody, polypeptide or other bioconjugate, or fragment thereof, can be administered to a subject and allowed to accumulate at a target site. When a targeted nanoparticle with a biotinylated surface is used, an avidin linker molecule, which attaches to the biotinylated targeting

ligand can be administered to the subject. Then, a targeted nanoparticle with a biotinylated shell can be administered to the subject. The targeted nanoparticle binds to the avidin linker molecule, which is bound to the biotinylated targeting ligand, which is itself bound to the desired target. In this way, a three step method can be used to target nanoparticles to a desired target. The targeting ligand can bind to all of the desired targets detailed above as would be clear to one skilled in the art.

Nanoparticles, including targeted nanoparticles, can also comprise a variety of markers, detectable moieties, or labels. Thus, for example, a nanoparticle equipped with a targeting ligand attached to its surface can also include another detectable moiety or label. As used herein, the term "detectable moiety" is intended to mean any suitable label, including, but not limited to, enzymes, fluorophores, biotin, chromophores, radioisotopes, colored particles, electrochemical, chemical-modifying or chemiluminescent moieties. Common fluorescent moieties include fluorescein, cyanine dyes, coumarins, phycoerythrin, phycobiliproteins, dansyl chloride, Texas Red, and lanthanide complexes. Of course, the derivatives of these compounds are included as common fluorescent moieties.

The detection of the detectable moiety can be direct provided that the detectable moiety is itself detectable, such as, for example, in the case of fluorophores. Alternatively, the detection of the detectable moiety can be indirect. In the latter case, a second moiety reactable with the detectable moiety, itself being directly detectable can be employed.

A composition, including at least one nanoparticle, can be administered to a subject orally, parenterally (e.g., intravenously), by intramuscular injection, by intraperitoneal injection, transdermally, extracorporeally, topically or the like. Parenteral administration of a composition, if used, is generally characterized by injection. Injectables can be prepared in conventional forms, either as liquid solutions or suspensions, solid forms suitable for solution of suspension in liquid prior to injection, or as emulsions.

The compositions, including nanoparticles, can be used in combination with a pharmaceutically acceptable carrier. By "pharmaceutically acceptable" is meant a material that is not biologically or otherwise undesirable, i.e., the material can be administered to a subject, along with the nanoparticle, without causing any undesirable biological effects or interacting in a deleterious manner with any of the other components of the pharmaceutical composition in which it is contained. The carrier would naturally be selected to minimize any degradation of the active ingredient and to minimize any adverse side effects in the subject, as would be well known to one of skill in the art.

Suitable carriers and their formulations are described in Remington: The Science and Practice of Pharmacy (19th ed.) ed. A. R. Gennaro, Mack Publishing Company, Easton, Pa. 1995. Typically, an appropriate amount of a pharmaceutically-acceptable salt is used in the formulation to render the formulation isotonic. Examples of the pharmaceutically-acceptable carrier include, but are not limited to, saline, Ringier's solution and dextrose solution. The pH of the solution is preferably from about 5.0 to about 8.0, and more preferably from about 7.0 to about 7.5. As described above compositions can be administered intravascularly. Administered compositions can include carriers, thickeners, diluents, buffers, preservatives, surface active agents and the like in addition to the composition of choice. Administered compositions can also include one or more active ingredients such as antimicrobial agents, anti-inflammatory agents, anesthetics, and the like.

When used in the described methods, an effective amount of one of the compositions, including the nanoparticles, of the present invention can be determined by one skilled in the art. The specific effective dose level for any particular subject can depend upon a variety of factors including the type and location of the target site, activity of the specific composition employed, the specific composition employed, the age, body weight, general health, sex and diet of the subject, the time of administration, the route of administration, the rate of excretion of the specific composition employed, the duration of the treatment, drugs used in combination or coincidental with the specific composition employed, and like factors well known in the medical arts. For example, it is well within the skill of the art to start doses of the composition at levels lower than those required to achieve the desired diagnostic or imaging effect and to gradually increase the dosage until the desired effect is achieved. If desired, an effective dose can be divided into multiple doses for purposes of administration.

Depending on the exemplary factors above, on the composition used, on the intended target site for the composition, and whether active or passive targeting of the described compositions is used, the time between administration of the described compositions and the detection of the described nanoparticles within the subject can vary. For example, detection of the described nanoparticles can be performed at one or more time seconds, minutes, hours, days, and/or weeks after administration of the compositions to the subject. When and how frequently methods of detection of an administered composition are performed can be determined by one skilled in the art through routine administration and detection.

Also provided herein are systems for detecting a cell or metallic composition. An exemplary system comprises a magnet for applying a magnetic field to a cell and a phase sensitive optical coherence tomographic imaging modality for detecting the cell and/or metallic composition. The phase sensitive optical coherence tomographic imaging modality can comprise a probe for transmitting and receiving light energy to and from the cell. The probe can be an intravascular probe.

The phase sensitive optical coherence tomographic imaging modality included in the system can comprise a light source, a light splitter, a probe and a reference reflector. Light energy generated by the light source can be transmitted to and split by the splitter for transmission to the reference reflector and to the probe. The probe can be configured to transmit at least a portion of the light energy transmitted thereto into a target cell and to receive reflected light energy from the target cell and the reference reflector can be configured to reflect at least a portion of the light energy transmitted thereto. The system can further include a processor for processing reflected light energy from the reference reflector and light energy received by the probe to produce a phase sensitive optical coherence tomography image. The reference reflector can be located in the probe.

Although the exemplary systems described below and shown in FIGS. 2 and 4 indicate a multitude of fibers in the sample path, the described systems and methods are not intended to be limited to embodiments having a multitude of fibers. Thus, systems comprising one fiber and methods of using such exemplary systems are covered. Optionally, an exemplary system comprises a probe having a single optical fiber and a rotary reflector in optical communication with the single optical fiber.

FIG. 1 is a block diagram illustrating an exemplary system 100 that can be used for performing the disclosed imaging methods. FIG. 2 is a block diagram illustrating an alternative exemplary system 200 for performing the disclosed imaging

methods. FIG. 3 is schematic diagram illustrating portions of the system of FIG. 1. FIG. 4 is a schematic diagram illustrating portions of the system of FIG. 2. These exemplary OCT systems are only examples of phase sensitive spectral domain OCT systems and are not intended to suggest any limitation as to the scope of use or functionality of OCT architectures. Neither should the OCT systems be interpreted as having any dependency or requirement relating to any one or combination of components illustrated in the exemplary OCT systems.

The exemplary OCT systems of FIGS. 1 and 2, 100 and 200 respectively, include a general-purpose computing device in the form of a computer 101, which is shown schematically in FIG. 3 as 311 and is shown schematically in FIG. 4 as 416. The components of the computer 101 can include, but are not limited to, one or more processors or processing units 103, a system memory 112, and a system bus 113 that couples various system components including the processor 103 to the system memory 112.

The system bus 113 represents one or more of several possible types of bus structures, including a memory bus or memory controller, a peripheral bus, an accelerated graphics port, and a processor or local bus using any of a variety of bus architectures. By way of example, such architectures can include an Industry Standard Architecture (ISA) bus, a Micro Channel Architecture (MCA) bus, an Enhanced ISA (EISA) bus, a Video Electronics Standards Association (VESA) local bus, and a Peripheral Component Interconnects (PCI) bus also known as a Mezzanine bus. This bus, and all buses specified in this description can also be implemented over a wired or wireless network connection. The bus 113, and all buses specified in this description can also be implemented over a wired or wireless network connection and each of the subsystems, including the processor 103, a mass storage device 104, an operating system 105, an image construction software 106, a nanoparticle movement image construction software 107, light signal data 108, the system memory 112, an OCT input interface 111, an OCT output interface 110, a display adapter 109, a display device 127, a human interface device 102, and a digital image capture device 117, can be contained within one or more remote computers (not shown) at physically separate locations, connected through buses of this form, in effect implementing a fully distributed system.

The computer 101 can include a variety of computer readable media. Such media can be any available media that is accessible by the computer 101 and includes both volatile and non-volatile media, removable and non-removable media.

The system memory 112 includes computer readable media in the form of volatile memory, such as random access memory (RAM), and/or non-volatile memory, such as read only memory (ROM). The system memory 112 typically contains data such as light signal data 108 and/or program modules such as operating system 105, image construction software 106 and nanoparticle movement (or cellular membrane tension level or internal strain field change) image construction software 107 that are immediately accessible to and/or are presently operated on by the processing unit 103. Throughout this application the disclosed methods, compositions and apparatuses for detecting a cell and/or a metallic composition are described herein variously by reference to metallic particle movement, cellular movement, changes in cellular tension level, changes in internal strain field of a cell, and change in neighboring or surrounding cells and/or tissues (s). It will be understood that description of various aspects of the disclosed methods, compositions and apparatuses by reference to detecting one or more of metallic particle movement, cellular movement, changes in cellular tension level,

changes in internal strain field of a cell, and change in neighboring or surrounding cells and/or tissues(s) constitutes description of that aspect of the disclosed methods, compositions and apparatuses to the non-referenced detection of metallic particle movement, cellular movement, changes in cellular tension level, changes in internal strain field of a cell, and change in neighboring or surrounding cells and/or tissues (s), unless the context clearly indicates otherwise. Thus, nanoparticle movement image construction software can also include or alternatively include cellular movement, changes in cellular tension level, changes in internal strain field of a cell, and change in neighboring or surrounding cells and/or tissues(s) image construction software.

The computer 101 can also include other removable/non-removable, volatile/non-volatile computer storage media. By way of example, FIG. 1 illustrates a mass storage device 104 which can provide non-volatile storage of computer code, computer readable instructions, data structures, program modules, and other data for the computer 101. For example, a mass storage device 104 can be a hard disk, a removable magnetic disk, a removable optical disk, magnetic cassettes or other magnetic storage devices, flash memory cards, CD-ROM, digital versatile disks (DVD) or other optical storage, random access memories (RAM), read only memories (ROM), electrically erasable programmable read-only memory (EEPROM), and the like.

Any number of program modules can be stored on the mass storage device 104, including by way of example, an operating system 105, image construction software 106, nanoparticle movement (or cellular membrane tension level or internal strain field change) image construction software 107, and light signal data 108. Each of the operating system 105, image construction software 106, nanoparticle movement (or cellular membrane tension level or internal strain field change) image construction software 107, light signal data 108 (or some combination thereof) can include elements of the programming image construction software 106 and the nanoparticle movement (or cellular membrane tension level or internal strain field change) image construction software 107.

A user can enter commands and information into the computer 101 via an input device (not shown). Examples of such input devices include, but are not limited to, a keyboard, pointing device (e.g., a "mouse"), a microphone, a joystick, a serial port, a scanner, and the like. These and other input devices can be connected to the processing unit 103 via a human machine interface 102 that is coupled to the system bus 113, but can be connected by other interface and bus structures, such as a parallel port, game port, or a universal serial bus (USB).

A display device 127 can also be connected to the system bus 113 via an interface, such as a display adapter 109. For example, a display device can be a monitor. In addition to the display device 127, other output peripheral devices can include components such as speakers (not shown) and a printer (not shown) which can be connected to the computer 101 via an input/output interface (not shown).

The computer 101 can operate in a networked environment using logical connections to one or more remote computing devices (not shown). By way of example, a remote computing device can be a personal computer, portable computer, a server, a router, a network computer, a peer device or other common network node, and so on.

Logical connections between the computer 101 and a remote computing device (not shown) can be made via a local area network (LAN) and a general wide area network (WAN). Such networking environments are commonplace in offices, enterprise-wide computer networks, intranets, and the Inter-

net. In a networked environment, image construction software **106**, nanoparticle movement (or cellular membrane tension level or internal strain field change) image construction software **107** and light signal data **108** depicted relative to the computer **101**, or portions thereof, can be stored in a remote memory storage device (not shown). For purposes of illustration, application programs and other executable program components such as the operating system are illustrated herein as discrete blocks, although it is recognized that such programs and components reside at various times in different storage components of the computing device **101**, and are executed by the data processor(s) of the computer.

An implementation of the image construction software **106** and the nanoparticle movement (or cellular membrane tension level or internal strain field change) image construction software **107** can be stored on or transmitted across some form of computer readable media. Computer readable media can be any available media that can be accessed by a computer. By way of example, and not limitation, computer readable media can comprise "computer storage media" and "communications media." "Computer storage media" include volatile and non-volatile, removable and non-removable media implemented in any method or technology for storage of information such as computer readable instructions, data structures, program modules, or other data. Computer storage media includes, but is not limited to, RAM, ROM, EEPROM, flash memory or other memory technology, CD-ROM, digital versatile disks (DVD) or other optical storage, magnetic cassettes, magnetic tape, magnetic disk storage or other magnetic storage devices, or any other medium which can be used to store the desired information and which can be accessed by a computer.

The light signal data **108** can enter the computer **101** via the OCT input interface **111**. The OCT output interface can be IEEE-488, IEEE-1394, Universal Serial Bus (USB), or the like. The light signal data **108** can be stored in mass storage device **104** and transferred to system memory **112** as light signal data **108** to be used by image construction software **106** and nanoparticle movement (or cellular membrane tension level or internal strain field change) image construction software **107**.

The OCT output interface **110** connects the computer **101** to a magnet control **114**. This connection can allow a user to regulate the current sent to a magnet **115** and a magnet **116** by the magnet control **114**. The magnet control **114** directs current flow into the magnets **115** or **116**. The magnet control **114** can work in conjunction with a line scan camera **139** so that a user-specified field pulse sequence is present at the scanning site.

FIG. 1 illustrates an example of a Phase Sensitive OCT system **100**. The Phase Sensitive OCT system **100** can be utilized in conjunction with the computer and network architectures described above.

The Phase Sensitive OCT system **100** can include a general-purpose computing device in the form of a computer **101** which is shown schematically in FIG. 3 as **311**, and all subsystems of the computer **101**, as previously described. The Phase Sensitive OCT system **200** can also include, as previously described, a display device **127**, a magnet control **114**, and a magnet **114** and/or a magnet **115**.

Light energy can be generated by a light source **117**, which is shown schematically in FIG. 3 as **301**. The light source **117** can be a broadband laser light source coupled into optical fiber emitting light energy over a broad range of optical frequencies. For example, the range can be from about 400 nanometers to about 1600 nanometers. The light energy can be emitted over a multiplicity of optical wavelengths or fre-

quencies. As used herein, optical fiber can refer to glass or plastic wire or fiber. Optical fiber is indicated on FIGS. 1, 2, 3, and 4 as lines connecting the various blocks of the figures. Where light energy is described as "passing," "traveling," "returning," "directed," or similar movement, such movement can be via optical fiber.

A fraction of the generated light energy passes from the light source **117** into an optical spectrum analyzer **118**. The optical spectrum analyzer **118** measures optical frequency as the light energy is emitted from the light source **117** as a function of time. The optical spectrum analyzer **118** samples a portion of the light emitted by the light source **117**. The optical spectrum analyzer **118** monitors the power spectral density of light entering the splitter **119**. The remaining fraction of light energy from the light source **117** passes into a splitter **119** which is shown schematically in FIG. 3 as **302**. The splitter **119** can be a device with four ports **312**, **314**, **316**, **318** on schematic diagram FIG. 3. Port 1 (**312**) allows light energy to enter the splitter **119**. Ports 2 (**314**) and 3 (**316**) allow light energy to leave and re-enter the splitter **119**. Port 4 (**318**) allows light energy to leave the splitter **119**. The splitter **119** couples the light into Port 1 (**312**). The splitter **119** divides the light according to a pre-determined split ratio selected by a user. For example, the split ratio can be 50/50 wherein half of the light energy entering the splitter **119** at Port 1 (**312**) exits the splitter **119** through Port 2 (**314**) and half exits the splitter **119** through Port 3 (**316**). In another non limiting example, the split ratio can be 60/40 wherein 60% of the light energy passes through Port 2 (**314**) and 40% of the light energy passes through Port 3 (**316**).

A fraction of the light energy (determined by the split ratio) that exits the splitter **119** through Port 2 (**314**) travels to a reference reflector surface **120** which is shown schematically in FIG. 3 as **303**. The light energy is reflected from the reference reflector surface **120** back to the splitter **119** into Port 2 (**314**). The reference reflector can be, by way of example, but not limitation, a planar metallic mirror or a multilayer dielectric reflector with a specified spectral amplitude/phase reflectivity. The remaining fraction of light that entered splitter **119** through Port 1 (**312**) exits splitter **119** through Port 3 (**316**) and enters an OCT probe **122** which is shown schematically in FIG. 3 as **304**. The OCT probe **122** can be a turbine-type catheter as described in Patent Cooperation Treaty application PCT/US04/12773 filed Apr. 23, 2004 which claims priority to U.S. provisional application 60/466,215 filed Apr. 28, 2003, each herein incorporated by reference for the methods, apparatuses and systems taught therein. The OCT probe **122** can be located within a subject **121** to allow light reflection off of subject **121** tissues, which is shown schematically in FIG. 3 as **305** and nanoparticles **123** which are shown schematically in FIG. 3 as **306**.

The light energy that entered OCT probe **122** is reflected off of the tissue of subject **121** and nanoparticles **123**. The reflected light energy passes back through the OCT probe **122** into the splitter **119** via Port 3 (**316**). The reflected light energy that is returned into Port 2 (**314**) and Port 3 (**316**) of the splitter **119** recombines and interferes according to a split ratio. The light recombines either constructively or destructively, depending on the difference of pathlengths. A series of constructive and destructive combinations of reflected light can be used to create an interferogram (a plot of detector response as a function of optical path length difference($c\tau$) or optical time-delay (τ)). Each reflecting interface from the subject **121** and the nanoparticles **123** can generate an interferogram. The splitter **119** can recombine light energy that is returned through Port 2 (**314**) and Port 3 (**316**) so that the light energies interfere. The light energy is recombined in the reverse of the

23

split ratio. For example, if a 60/40 split ratio, only 40% of the light energy returned through Port 2 (314) and 60% of the light energy returned through Port 3 (316) would be recombined. The recombined reflected light energy is directed out Port 4 (318) of the splitter 119 into a coupling lens 137 which is shown schematically in FIG. 3 as 308. The coupling lens 137 receives light from the output of the splitter 119 and sets the beam etendue (beam diameter and divergence) to match that of the optical spectrometer 138. The coupling lens 137 couples the light into an optical spectrometer 138 which is shown schematically in FIG. 3 as 309. The optical spectrometer 138 can divide the recombined reflected light energy light into different optical frequencies and direct them to different points in space which are detected by a line scan camera 139 which is shown schematically in FIG. 3 as 310. The line scan camera 139 performs light to electrical transduction resulting in digital light signal data 108. The digital light signal data 108 is transferred into the computer 101 via the OCT Input interface 111. Interface between the line scan camera 139 and computer 101 can be, for example, IEEE-488, IEEE-1394, Universal Serial Bus (USB), or the like. The digital light signal data 108 can be stored in the mass storage device 104 or system memory 112 and utilized by the image construction software 106 and the nanoparticle movement (or cellular membrane tension level or internal strain field change) image construction software 107.

The preceding exemplary phase sensitive OCT system is only one example of the contemplated systems for imaging tissues and nanoparticles. Variations in layout and equipment known to one skilled in the art are also contemplated. Another example of a phase sensitive OCT system that can be used to perform the method of the invention is illustrated in FIG. 2.

FIG. 2 is an exemplary block diagram of a Multi-Channel Phase Sensitive OCT system 200. The exemplary Multi-Channel Phase Sensitive OCT system 200 can include a general-purpose computing device in the form of the computer 101, which is shown schematically in FIG. 4 as 416, and all subsystems of the computer 101, as described herein. The exemplary multi-channel Phase Sensitive OCT system 200 can also include, as previously described, a display device 127, a magnet control 114, and a magnet 114 or a magnet 115.

Light energy is generated by a light source 212, which is shown schematically in FIG. 4 as 401. The light source 212 can be a narrow band tunable laser light source wherein the optical wavelengths generated range from about 400 nanometers to about 1600 nanometers. Appropriate selection of a range of optical wavelengths can be readily determined by one skilled in the art. For example, if light energy is to go through substantial water path, i.e., deep tissue, then an operator can select longer optical wavelengths. For example, 1300-1600 nanometers. The light spectrum is continuously varied in time, over a specified spectral region. A fraction of the light energy passes from the light source 212 into an optical spectrum analyzer 118. The optical spectrum analyzer 118 samples a portion of the light emitted by the light source 212. The optical spectrum analyzer 111 monitors the power spectral density of light entering the circulator 201. The optical spectrum analyzer 118 can measure optical frequency as it is emitted from the light source 212 as a function of time. The remaining fraction of light energy generated by the light source 212 passes into a fiber circulator 201, which is shown schematically in FIG. 4 as 402. The fiber circulator 201 can comprise three ports, designated Port 1, Port 2, and Port 3, which are shown schematically in FIG. 4 as 418, 420, and 422 respectively. Light energy can enter Port 1 (418). Light energy can exit and re-enter Port 2 (420). Light energy can exit Port 3. The fiber circulator 201 can recombine light

24

energy that re-enters via Port 2 (420). Light energy from the light source 212 passes into the fiber circulator 201 through Port 1 (418). The light energy exits the fiber circulator 201 through Port 2 (420) and enters an OCT probe 207, which is shown schematically in FIG. 4 as 403. The light energy is coupled to a collimator lens 202, which is shown schematically in FIG. 4 as 404. The collimator lens 202 focuses the light emitted from the fiber at a point infinitely far from the fiber tip.

The light energy is collimated into a lens array 203, which is shown schematically in FIG. 4 as 405. The lens array 203 can comprise a lattice of microlenses or lenslets, which are shown schematically in FIG. 4 as 422. The number of microlenses in the lens array 203 can be readily determined by one skilled in the art. For each microlens, there is a fiber channel 204, which is shown schematically in FIG. 4 as 406, that is coupled to the microlens. Fiber channels 204 are optical waveguides that confine and guide light along a path. The fiber channels 204 can be varied in length. Choosing an appropriate length for the fiber channels 204 is known to one skilled in the art. The difference in the length between fiber channels 204 can be from about one and a half to about ten times the scan depth in the tissue of a subject 121. This variable length can allow demultiplexing light signal detected from the channels. A fraction of the light energy transmitted into the fiber channels 204 is reflected from a reference reflector surface 120 back into the fiber channels 204, through the lens array 203, into the collimator lens 202 and into the fiber circulator 201. This reflected light energy can serve as a reference reflection. The light energy that is not reflected back from the reference reflector surface 120 passes through the reference reflector surface 120 and onto an imaging lens 205, which is shown schematically in FIG. 4 as 407. The imaging lens 205 images the light energy from the tips of the fiber channels 204 onto the tissue of the subject 121. The light energy passes through the imaging lens 205 onto a reflector surface 206, which is shown schematically in FIG. 4 as 408, which turns the light energy 90 degrees. This allows the light energy to be reflected out radially inside a tissue. There is one reflector surface 206 for each fiber channel 204. The light energy that is turned 90 degrees by the reflector surface 206 is back reflected off of the tissue of subject 121, which is shown schematically in FIG. 4 as 409, and nanoparticles 123, which is shown schematically in FIG. 4 as 410.

The light is reflected from the tissue of subject 121 and the nanoparticles 123. The light energy strikes the reflector surface 206 and is turned back 90 degrees. The light energy is then coupled by the imaging lens 205 through the reference reflector surface 120 and back into each fiber channel 204. The light energy reflected from the nanoparticles 123 and the tissue of subject 121 recombines and interferes with the light reflected from the reference reflector surface 120 in the fiber channels 204. The recombined light energy can be coupled back into the lens array 203 through the collimator lens 202 and back into Port 2 (420) of the fiber circulator 201. The recombined light energy exits the fiber circulator 201 through Port 3 (422). A coupling lens 208, which is shown schematically in FIG. 4 as 412, couples the recombined light energy from the fiber circulator 201 into a photo receiver 209, which is shown schematically in FIG. 4 as 413. The photo receiver 209 converts the light energy signal into a voltage signal that is proportional to the number of photons contained in the recombined light energy. The voltage signal passes from the photo receiver 209 into a pre/amp 210, which is shown schematically in FIG. 4 as 414. The pre/amp 210 takes the voltage signal and amplifies it. The amplified voltage signal enters an A/D converter 211, which is shown schematically in FIG. 4 as

415. The A/D converter 211 digitizes the voltage signal. This digital light signal data then enters the computer 101 through the OCT input interface 111. The digital light signal data 108 can be stored in the mass storage device 104 or system memory 112 and utilized by the image construction software 106 and the nanoparticle movement (or cellular membrane tension level or internal strain field) image construction software 107.

The method can further comprise generating light energy for at least two successive sweeps of light energy. A sweep is an emission of light from a light source across a range of optical frequencies. Multiple sweeps can be combined with application of a magnetic field to generate images with and without a magnetic field applied.

The method can further comprise applying a magnetic field to the subject for each of the successive sweeps of the light energy wherein the strength of the magnetic field applied in a sweep is greater than the strength of the magnetic field from the preceding sweep and wherein the magnetic field causes movement of at least one of the metallic nanoparticles. The method can further comprise applying the magnetic field from a source external to the subject or from a source internal to the subject. A coil generating the magnetic field can be integrated into a catheter or can be external to the subject of the scan.

As shown in FIGS. 1 and 2, a non-uniform magnetic field can be applied to the tissue of subject 121 and the nanoparticles 123. The non-uniform magnetic field can be applied by the magnet 116, which is shown schematically in FIG. 3 as 307 and schematically in FIG. 4 as 411, which can be a magnet internal to the OCT probe 122 or the OCT probe 207 or the non-uniform magnetic field can be applied externally to the subject 121 by magnet 115. Magnets 115 and magnet 116 are both controlled by magnet control 114. The magnet control can provide the current source to power magnet 115 and magnet 116 and is under the control of the computer 101. The magnet control 114 interfaces with the computer 101 through the OCT output interface 110. The magnet control 114 can interface with the computer 101 via IEEE-488, IEEE-1394, Universal Serial Bus (USB), or the like.

The method can further comprise processing the received light energy to produce a phase sensitive OCT image. The image produced can have a phase resolution of at least 30 nanometers (nm). Phase resolution is defined as the phase delay of the light signal returning from the tissue scanned. For example, the image can have a phase resolution of about at least 30nm, 25 nm, 20 nm, 15 nm, 10 nm, 5 nm, 4 nm, 3 nm, or 2 nm.

The processing of the received light energy can be performed by software components. The image construction software 106 and the nanoparticle movement (or cellular membrane tension level or internal strain field) image construction software 107 can be described in the general context of computer-executable instructions, such as program modules, being executed by one or more computers or other devices. Generally, program modules include computer code, routines, programs, objects, components, data structures, etc. that perform particular tasks or implement particular abstract data types. The image construction software 106 and the nanoparticle movement (or cellular membrane tension level or internal strain field) image construction software 107 can also be practiced in distributed computing environments where tasks are performed by remote processing devices that are linked through a communications network. In a distributed computing environment, program modules can be located in both local and remote computer storage media including memory storage devices.

The image construction software 106 can generate an image of the tissue of subject 121 from the light signal data 108. The image construction software 106 can receive the light signal data 108 and can perform a time-frequency transform (e.g. Fourier transform) on the light signal data 108 generating amplitude and phase data. The amplitude and phase data (optical path length difference ($\epsilon\tau$) or optical time-delay (τ)) can be separated into discrete channels and a plot of intensity vs. depth (or amplitude vs. depth) can be generated for each channel. Such a plot is known in the art as an "A" scan. The composition of all the "A" scans can comprise one image.

The nanoparticle movement (or cellular membrane tension level or internal strain field) image construction software 107 generates an image of the movement of the nanoparticles 123 from the light signal data 108. The nanoparticle movement (or cellular membrane tension level or internal strain field) image construction software 107 receives the light signal data 108 for at least two successive sweeps of the light source 117 or the light source 212 and performs a Fourier transform on the light signal data 108 generating amplitude and phase data. The amplitude and phase data can be separated into discrete channels, one channel for each fiber channel 204, and a plot of phase vs. depth (optical time-delay (τ)) can be generated for each channel. Points of nanoparticle 123 movement are identified when phase at a given depth changes between two successive sweeps of the light source 117 or the light source 212 corresponding to two applied magnetic field strengths.

Optionally, additional information can be extracted from the light signal data 108 to generate additional images. The light signal data 108 can be further processed to extract the Doppler frequency shift as is readily known to one skilled in the art. The light signal data 108 can also be further processed to generate a Stokes parameter polarimetric image when used in conjunction with polarization detectors (not shown) and polarizing lenses (not shown) to extract polarization data from the light signal 108 as is readily known to one skilled in the art.

EXAMPLES

The following examples are put forth so as to provide those of ordinary skill in the art with a complete disclosure and description of how the compositions, compositions, articles, devices, systems, and/or methods claimed herein are made and evaluated, and are intended to be purely exemplary and are not intended to limit the scope of compositions, compositions, articles, devices, systems, and/or methods. Efforts have been made to ensure accuracy with respect to numbers (e.g., amounts, temperature, etc.), but some errors and deviations should be accounted for. Unless indicated otherwise, parts are parts by weight, temperature is in ° C. or is at ambient temperature, and pressure is at or near atmospheric.

Example 1

A solenoid coil with a ferrite core was used to apply a sinusoidal magnetic field to tissues taken from the liver of an ApoE $-/-$ knockout mouse. One mouse was loaded with magnetic nanoparticles one week before imaging while an unloaded mouse served as a control. FIG. 5a shows a solenoid drive signal (top) and optical pathlength change (bottom) observed in mouse loaded with nanoparticles. FIG. 5b shows a solenoid drive signal (top) and optical pathlength change (bottom) observed in control mouse (no nanoparticles). These data demonstrate that iron oxide particles that have been ingested by macrophages in livers and spleens of the mice.

Moreover, the particles have put in motion with a magnet and detected with differential phase OCT using the systems and methods described herein.

To calculate magnetic field strength a finite element method (FEM) can be used. Maxwell equations subjected to certain boundary conditions can be used to solve low-frequency magnetostatic problems. The use and solution of Maxwell equations are described in, for example, Monk P., Finite Element Methods for Maxwell's Equations, Oxford University Press, 2003, which is incorporated in its entirety by reference.

Maxwell equations can be written as:

$$\nabla \times H = J + \frac{\partial D}{\partial t} \quad (1.1)$$

$$\nabla \times E = -\frac{\partial B}{\partial t} \quad (1.2)$$

$$\nabla \cdot H = \rho \quad (1.3)$$

$$\nabla \cdot B = 0 \quad (1.4)$$

In case of magnetostatic problems

$$\left(\frac{\partial D}{\partial t} = 0\right),$$

the magnetic field (H) and magnetic flux density (B) are satisfied with following equations:

$$\nabla \times H = J \quad (1.5)$$

$$\nabla \cdot B = 0 \quad (1.6)$$

B and H are Subject to a generalized constitutive relation:

$$B = \mu_0(H + M) \quad (1.7)$$

Finite element methods (FEM) used magnetic vector potential (A) to find magnetic field strength.

$$B = \nabla \times A \quad (1.8)$$

Equation (1.5) can be rewritten as

$$\nabla \times (\mu_0^{-1} \nabla \times A - M) = J \quad (1.9)$$

From equation (1.9), magnetic field strength and flux density can be solved. The symbols and unit for electromagnetic quantities for solving FEM problems include:

H: Magnetic field (Ampere/m)

E: Electric field (Volt/meter)

B: Magnetic flux density (Tesla)

D: Electric flux density (Coulomb/meter²)

A: Magnetic potential (Weber/meter)

M: Magnetization (Ampere/meter)

μ_0 : Permeability of vacuum = $4\pi \times 10^{-7}$ (H/m)

$$\Delta \cdot B = \text{div} B = \frac{\partial}{\partial x} B_x + \frac{\partial}{\partial y} B_y + \frac{\partial}{\partial z} B_z \quad (\nabla \cdot B \text{ is divergence of } B)$$

Magnetic fields of between about 1.5 and 2.0 Tesla were used to cause movement of the nanoparticles. Magnetic fields between about 1.0 and 9.0 Tesla can also be used. The magnetic field used is typically higher if the tissue of interest comprises a greater number of nanoparticles or iron, when compared to tissue with fewer nanoparticles or iron.

Example 2

Colloidal suspensions of SPIO nanoparticles are tissue-specific MRI contrast agents approved by the United States Food and Drug Administration (FDA) for human use in 1997. SPIO particles are also known as Ferumoxides or AMI-25 and their trade name is Feridex® I.V. (USA) and Endorem® (EU). Mean core diameter of these particles is 20 nm and total aggregation diameter is about 100 nm. SPIO nanoparticles comprise nonstoichiometric magnetite crystalline cores, iron, and dextran T-10 coating that is used to prevent aggregation and stabilization in the liver. 80% of injected dose of SPIO nanoparticles accumulate in tissue based macrophages (Kupffer cells) due to the relatively short blood half life compared to ultrasmall SPIO nanoparticles. Uptake of SPIO nanoparticles by macrophage cells is directly proportional to the intravenous injection (IV) concentration, blood half life, and core size.

To evaluate magnetic force on superparamagnetic (SPIO) nanoparticles, magnetic potential energy, U, can be used to calculate force due to application of an external magnetic flux density (B).

$$U = -\frac{1}{2} m \cdot B \quad (1)$$

If a magnetic material is exposed to an external magnetic flux density, B, the individual particles have overall response determined by the magnetic moment, m. The magnetic flux density on magnetic nanoparticles can be written:

$$B = \mu_0(H + M) \quad (2)$$

where μ_0 ($4\pi \times 10^{-7}$ H/M) is the permeability of free space, and M is the magnetic moment per unit volume and H is magnetic field strength. The magnetic moment, m, acting on magnetic volume, V is given by, $m = MV$. Magnetization of magnetic particles can be classified in terms of the standard relation $M = \chi H$. Therefore, magnetic moment m becomes:

$$m = MV = \chi_s V H = \chi_s V B / \mu_0 \quad (3)$$

In Eq.(3), susceptibility of the SPIO particles χ_s is dimensionless in SI units and given by dipole density for each paramagnetic material and is an important parameter characterizing magnetic properties of SPIO nanoparticles. From Eq.(1), magnetic energy U, of a SPIO nanoparticles in external magnetic field is given by,

$$U = -\frac{1}{2} m \cdot B = -\frac{\chi_s V}{2\mu_0} B^2. \quad (4)$$

Magnetic force acting on SPIO nanoparticles becomes:

$$F = -\nabla U = \nabla \left(\frac{\chi_s V}{2\mu_0} B^2 \right) = \chi_s V \nabla \left(\frac{B^2}{2\mu_0} \right). \quad (5)$$

A sinusoidal magnetic flux density that is principally along the z-direction was assumed. Hence, $\vec{B}(x, y, z, t) = \sin(2\pi f_m t) B_z(z) \hat{k}$ and the magnetic force F_z acting on nanoparticles in the z-direction is given by

$$\sum F_z = m \frac{\partial^2 z(t)}{\partial t^2} = F_m - kz(t) - r \frac{\partial z}{\partial t} \quad (6)$$

$$\sum F_z = \frac{\chi_s V_s}{2\mu_0} [1 - \cos(4\pi f_n t)] B_z(z) \frac{\partial B_z}{\partial z} - kz(t) - r \frac{\partial z}{\partial t}, \quad (7)$$

where F_m is magnetic force, f_n is the modulation frequency of the applied sinusoidal magnetic field, $kz(t)$ is an elastic restoring force, and

$$r \frac{\partial z}{\partial t}$$

is a viscous drag force that account for the viscoelastic properties of the local tissue environment. The negative sign of the viscous drag and restoring force indicates that this force is in opposite direction to movement $z(t)$. Equation 8 can be written by dividing by the mass, m .

$$\frac{\partial^2 z(t)}{\partial t^2} + \frac{kz(t)}{m} + \frac{r}{m} \frac{\partial z}{\partial t} = \frac{\chi_s V_s}{2m\mu_0} [1 - \cos(4\pi f_n t)] B_z(z) \frac{\partial B_z}{\partial z} \quad (8)$$

Equation 8 can be rewritten using the first terms in the Maclaurin series for the magnetic field,

$$\frac{\partial^2 z(t)}{\partial t^2} + \frac{r}{m} \frac{\partial z}{\partial t} + \frac{kz(t)}{m} \cong \frac{\chi_s V_s}{2m\mu_0} [1 - \cos(4\pi f_n t)] B_z(0) \frac{\partial B_z(0)}{\partial z} \quad (8)$$

Letting a

$$a = \frac{\chi_s V_s}{2m\mu_0} B_z(0) \frac{\partial B_z(0)}{\partial z},$$

$c=4\pi f_n$, the second order differential Eq. (8) can be written

$$\frac{\partial^2 z(t)}{\partial t^2} + \frac{r}{m} \frac{\partial z}{\partial t} + \frac{kz(t)}{m} = a[1 - \cos(ct)], \quad (9)$$

The Laplace transform can be used to solve the second order differential equation (9), assuming zero initial displacements and velocity to find;

$$s^2 Z(s) + \frac{r}{m} s Z(s) + \frac{k}{m} Z(s) = \frac{a}{s} - \frac{as}{(s^2 + c^2)} \quad (10)$$

$$Z(s) = \frac{\frac{a}{s} - \frac{as}{(s^2 + c^2)}}{\left(s^2 + \frac{r}{m}s + \frac{k}{m}\right)} = a \left(\frac{1}{\left(s^2 + \frac{r}{m}s + \frac{k}{m}\right)s} - \frac{s}{\left(s^2 + \frac{r}{m}s + \frac{k}{m}\right)} \right)$$

By computing the sum of the transforms, $Z(s)$ can be derived in Eq (10).

$$z(t) = \frac{ma \exp\left(-\frac{1}{2} \frac{tr}{m}\right) \left(\frac{c^2(km - r^2 - c^2 m^2) \cosh\left(\frac{1}{2} \frac{t(r^2 - 4km)^{\frac{1}{2}}}{m}\right) + c^2 r(3km - r^2 - c^2 m^2) \sinh\left(\frac{1}{2} \frac{t(r^2 - 4km)^{\frac{1}{2}}}{m}\right)}{(r^2 - 4km)^{\frac{1}{2}}} \right)}{(k(-2mkc^2 + c^2 r^2 + k^2 + c^4 m^2) - \cos(ct)k^2 + \cos(ct)c^2 mk - cr \sin(ct)k + \dots)} \quad (11)$$

The displacement $z(t)$ of nanoparticles can be found by using an inverse Laplace transform; the solution includes transient and steady state terms. The initial motion of magnetic nanoparticles is driven by a constant magnetic force and displays a damped transient motion before steady state motion dominates at twice the modulation frequency (f_n) of the applied sinusoidal magnetic field. Motion of the nanoparticles at double the modulation frequency originates from the magnetic force being proportional to the product of the field and field-gradient (Eq. 7).

Liver tissues from 12 week old ApoE^{-/-} high fat fed mice were utilized because they contain tissue based macrophages cells. The mice were injected via the jugular vein with either Feridex I. V. (Ferumoxides injectable solutions; Berelox Laboratories, Montville, N.J.) for intravenous administration (1.0, 0.1, and 0.01 mmol Fe/kg body weight) or saline and sacrificed 2 days post intravenous injection. The mice were euthanized with a lethal dose of Ketamine and Xylazine. After euthanizing, abdominal incisions were made to remove the entire liver from the mouse. Portions were cut using a microtome. Physical thickness of the liver samples was 1 mm and 0.5 cm×0.5 cm in lateral dimensions. After completion of the DP-OCT measurements, the mouse livers were embedded in 10% formalin acid, and processed for histology. 5 μm thick sections were cut and stained with Prussian blue to identify iron deposition in liver Kupffer cells in mouse liver tissues. To verify SPIO uptake by macrophage cells from histology slides, Image Pro Plus® (Mediacynergetics Inc., Silver Spring, Md.) was used to measure the total area of liver and accumulated area of SPIO aggregation containing Prussian blue positive.

FIGS. 6a and b shows a schematic diagram of a fiber-based dual channel differential phase optical coherence tomography (DP-OCT) system (a), and sample path configuration with a magnetic Field generator (b). The magnetic Field generator comprises a solenoid, signal generator and current amplifier. A dual-channel Michelson interferometer was used to measure differential phase between light backscattered from a sample by applying a sinusoidal focused magnetic field excitation. Partially polarized light from an optical semiconductor amplifier (AFC Technologies, Rancho Cordova, Calif., central wavelength $\lambda_0=1.31 \mu\text{m}$, FWHM=60 nm, optical coherence length=22 μm) is polarized and coupled into fast and slow axes of a polarization-maintaining (PM) fiber in the input port.

Optical path length change (Δp) in tissue can be calculated from the differential phase ($\Delta\phi$) and central wavelength of a broad-band light source ($\lambda_0=1,310 \text{ nm}$) between the two channels.

31

$$\Delta p = \frac{\lambda_0}{4\pi} \Delta \varphi \quad (13)$$

The displacement $z(t)$ of tissue-laden nanoparticles driven by a time (t) varying magnetic flux density can be derived the analytic OCT fringe expression,

$$I_f = 2\sqrt{I_R I_s} \cos\left[2\pi f_0 t + \frac{4\pi z(t)}{\lambda_0}\right] \quad (12)$$

Where I_R and I_s are the back scattered signals from the reference and sample arms, respectively. f_0 is the fringe carrier frequency, and $z(t)$ is the nanoparticles displacement. The OCT fringe signal can be expressed by the nanoparticles displacement equation (12). The two signals recorded from Channel 1 and 2 by the DP-OCT system can be used to measure nanoparticles displacement that represent relative surface tissue displacement between two scanning beams.

Finite element method (FEM) was used to design the magnetic field generator and evaluate space-time magnetic flux density. The magnetic field generator comprises a solenoid (Ledex 6EC, Saia-Burgess Inc., Vernon Hills, Ill.), a function generator (HP 33120A, Hewlett Packard Inc., Palo Alto, Calif.), a current amplifier, and a power supply. FEM calculations (Maxwell SV, Ansoft Inc., Pittsburgh, Pa.) and Teslometer® (Magnetometer(D, AlphaLab Inc., Salt Lake City, Utah) measurement indicated that the maximum magnetic flux density at a distance of 1.5 mm from the tip of the iron core was approximately 2 Tesla. The FEM simulation demonstrated that an iron core positioned along the centerline of the solenoid dramatically increased magnetic flux density at the target specimen. Magnetic field distributions from the FEM simulation showed the maximal and principal direction of the magnetic field strength was in the z-direction. The conical iron core provided focusing and substantially increased the magnetic field strength.

Differential phase OCT (DP-OCT) measurements were performed on isolated liver specimens taken from ApoE^{-/-} mice administrated with different SPIO doses (1.0, 0.1 and 0.01 mmol Fe/kg body weight) and saline control samples. FIG. 7 demonstrates measurements of transient optical path length change (Δp) in specimens at different SPIO doses (1.0, 0.1 mmol Fe/kg body weight) and saline control samples, in response to application of a sinusoidal varying focused magnetic field. FIG. 7(a) shows a magnetic field input ($f_m=2$ Hz), peak-to-peak voltage ($V_{pp}=4$) over a 1 second time period. The maximum magnetic field strength was 0.47 Tesla and maximal tissue displacement by optical path length change (Δp) was 2,273 nm in the 1.0 mmol Fe/kg iron-laden liver.

Compared to high dose specimens, 0.1 mmol Fe/kg iron-laden liver showed a maximum optical path length change (Δp) of 127 nm with additive noise visible in recorded signals.

Frequency response (4 Hz) of iron-laden livers (FIG. 7(b), (c)) was exactly twice the modulation frequency (2 Hz) as noted earlier. No significant displacement of SPIO nanoparticles was observed in either saline control liver specimens in the FIG. 7(d) or samples at the 0.01 mmol Fe/kg dose (not shown).

SPIO nanoparticle movement in the iron laden livers (0.1, and 1.0 mmol Fe/kg) was used to observe quantitatively the relationship between optical path length change (Δp) versus different applied magnetic field strengths (FIG. 8(a)). Input frequency used in this experiment was 2 Hz with amplitude from 2 to 8 V_{pp}. FIG. 8(b) shows magnetic flux density at the

32

same voltages as in FIG. 8(a). Magnitude of optical path length change (Δp) indicating movement of iron-laden liver depended directly on the SPIO dose concentration, and strength of the external magnetic field.

Optical path length change (Δp) at high frequency modulation (over 100 Hz) was negligible due to limited frequency response of the structures surrounding SPIO nanoparticles. Generally, optical path length change (Δp) due to nanoparticles movement in tissue increased with higher magnetic field strength.

Optical path length change (Δp) in the iron-laden liver (0.1 and 1.0 mmol Fe/kg) can be measured using a swept input frequency as shown in FIG. 9. FIG. 9(a) shows the magnetic field input with a swept frequency from 1 to 10 Hz over a 2 second time-period.

Magnitude of the optical path length change (Δp) was 2,318 nm in a high dose liver (1.0 mmol Fe/kg) and 177 nm in a low dose concentration (0.1 mmol Fe/kg), and magnetic field strength was 1.3 Tesla. The frequency response of the force acting on the iron-laden liver is exactly twice the externally applied modulated frequency in FIGS. 9(b) and (c). No significant displacement was observed in the saline control liver shown in FIG. 9(d) and 0.01 mmol Fe/kg liver specimens.

FIG. 10 illustrates SPIO nanoparticle movement measured by optical path length change (Δp) in a iron-laden mouse liver to observe quantitatively the relationship between magnetic response in tissue versus different applied magnetic field strengths with swept frequency ranging from 1~10 Hz over a 2 second time-period. Magnitude of optical path length change (Δp) was larger when input voltage was gradually increased from 2 to 10 V_{pp} during a frequency sweep. Corresponding magnetic field strength at these voltages was 1.24, 1.58, 1.71, 1.75 and 1.84 Tesla, respectively. For a given frequency sweep, maximum optical path length change (Δp) for 0.1 and 1.0 mmol Fe/kg iron-laden liver specimens was 3,700 nm and 750 nm, respectively, at 10 V_{pp}, and magnetic field of 1.84 Tesla.

SPIO nanoparticles were identified in histological specimens as blue granules from the Prussian blue stain of iron laden mouse livers. Compared to control liver specimens, iron laden specimens show significant iron accumulation evenly distributed in all observed areas. Although intracellular iron was also observed in control specimens, this natural iron was uniform and homogeneous rather than appearing in granular shapes as SPIO iron nanoparticles. Total SPIO iron area was 5.45% of the histology image as calculated by Image-Pro PLUS 5.1 software (Mediacynemetics Inc., Silver Spring, Md.).

Example 3

Optical path length change (Δp) in iron-laden rabbit arteries (0.1 Fe/kg) was measured in response to 2 Hz frequency sinusoidal input (FIG. 11). FIG. 11(a) shows the magnetic field input with a constant frequency at 2 Hz over a 2.5 second time-period. Magnitude of the optical path length change (Δp) indicated a transient and steady state response. Transient response is evident in the exponentially decaying oscillation in the observed measured optical path length change at times between 0.5-1.0 seconds. Steady state response is evident in the uniform oscillation in the measured optical path length change at times between 1.25-3.0 seconds. Transient response indicates a high frequency (40 Hz-80 Hz) "ringing" oscillation and a damping relaxation time of approximately 0.3 seconds. The steady state frequency response of the force

acting on the iron-ladell rabbit artery was exactly twice the externally applied modulated frequency in FIG. 11(b).

Throughout this application, various publications are referenced. The disclosures of these publications in their entireties are hereby incorporated by reference into this application in order to more fully describe the state of the art to which this invention pertains.

It will be apparent to those skilled in the art that various modifications and variations can be made in the present invention without departing from the scope or spirit of the invention. Other embodiments of the invention will be apparent to those skilled in the art from consideration of the specification and practice of the invention disclosed herein. It is intended that the specification and examples be considered as exemplary only, with a true scope and spirit of the invention being indicated by the following claims.

What is claimed is:

1. A method for detecting a cell, comprising:
applying a first magnetic field strength to the cell, wherein the cell comprises a cellular membrane and a magnetically susceptible material;
applying a second magnetic field strength to the cell, wherein the second magnetic field strength is different from the first magnetic field strength and interacts with the magnetically susceptible material to cause a change in the cell relative to interaction of the cell with the first magnetic field strength; and
detecting the cell by detecting the change in the cell, wherein the change is detected using a phase sensitive frequency domain optical coherence tomographic imaging modality including a common path interferometer during the application of at least one of the first and second magnetic field strengths.
2. The method of claim 1, wherein the change is selected from the group consisting of: movement of the cell, movement of the magnetically susceptible material, a change in the cellular membrane tension level, and a change in the internal strain field of the cell.
3. The method of claim 1, wherein the phase sensitive optical coherence tomographic imaging modality comprises using a probe for transmitting and receiving light energy to and from the cell.
4. The method of claim 3, wherein the probe further comprises a magnetic source for applying at least one of the first and second magnetic field strengths to the cell.
5. The method of claim 1, wherein at least one of the first and second magnetic field strengths is applied to the cell from a magnetic source located external to the probe.
6. The method of claim 1, wherein the magnetically susceptible material is located within the cell.
7. The method of claim 1, wherein the magnetically susceptible material is targeted to a location on the cellular membrane of the cell.
8. The method of claim 1, wherein the magnetically susceptible material has a non-zero magnetic susceptibility.
9. The method of claim 8, wherein the magnetically susceptible material comprises a material selected from the group consisting of iron oxide, iron, cobalt, nickel, and chromium.
10. The method of claim 1, wherein the magnetically susceptible material comprises a plurality of metallic nanoparticles.
11. The method of claim 10, wherein the nanoparticles are substantially spherical and have a diameter from about 0.1 nanometers (nm) to about 1000.0 nm.
12. The method of claim 10, wherein the nanoparticles are asymmetrical in shape.

13. The method of claim 12, wherein the largest cross sectional dimension of the nanoparticles is from about 0.1 nanometers (nm) to about 1000.0 nm in length.

14. The method of claim 9, wherein the cell is detected in vivo and the magnetically susceptible material is administered to the subject.

15. The method of claim 14, wherein the cell is a macrophage and wherein at least one nanoparticle is located within the macrophage.

16. The method of claim 15, wherein the macrophage is located in an atherosclerotic plaque within the subject.

17. The method of claim 15, wherein the macrophage is located within the eye of the subject.

18. The method of claim 14, wherein at least one of the nanoparticles is configured to localize to a target site within the subject.

19. The method of claim 18, wherein the target site is a neoplastic cell.

20. The method of claim 18, wherein the target site is an extracellular domain of a protein.

21. The method of claim 18, wherein the cell comprises the target site, and wherein the cell is located in the subject at an anatomical location selected from the group consisting of a lung, bronchus, intestine, stomach, colon, eye, heart, blood vessel, cervix, bladder, urethra, skin, muscle, liver, kidney, and blood.

22. The method of claim 18, wherein the cell comprises the target site and wherein the cell is selected from the group consisting of a neoplastic cell, a squamous cell, a transitional cell, a basal cell, a muscle cell, an epithelial cell, and a mucosal cell.

23. The method of claim 18, wherein the nanoparticle comprises an antibody or fragment thereof.

24. The method of claim 23, wherein the antibody or fragment thereof is conjugated to the surface of the nanoparticle.

25. The method of claim 18, wherein the nanoparticle comprises a peptide or a fragment thereof.

26. The method of claim 25, wherein the peptide or fragment thereof is conjugated to the surface of the nanoparticle.

27. The method of claim 1, further comprising the steps of capturing one or more lines of phase sensitive light energy data using the phase sensitive optical coherence tomography modality, and generating a phase sensitive optical coherence tomographic image from the one or more lines of phase sensitive light energy data captured using the phase sensitive optical coherence tomography modality, wherein at least one line of the one or more lines of phase sensitive light energy data is captured during the application of at least one of the first and second magnetic field strengths.

28. The method of claim 27, wherein the step of capturing one or more lines of phase sensitive light energy data comprises: generating light energy; transmitting at least a first portion of the generated light energy onto a reference reflector wherein at least a portion of the transmitted first portion of light energy is reflected by the reference reflector; transmitting at least a second portion of the generated light energy to contact the cell wherein at least a portion of the light energy that contacts the cell is reflected by the cell; receiving the light energy reflected by the reference reflector and by the cell; combining the received light energy from the cell and reference reflector, wherein the received light energy interferes; and processing the combined light energy to produce the phase sensitive optical coherence data line.

29. The method of claim 28, wherein movement of the cell is detected.

35

30. The method of claim 28, wherein a change in the cellular membrane's tension level or internal strain field is detected.

31. The method of claim 28, wherein the image produced has a phase sensitive resolution of at least about 30.0 nanometers (nm), 25.0 nm, 15.0 nm, 10.0 nm, 5.0 nm, 4.0 nm, 3.0 nm, or 2.0 nm.

32. The method of claim 27, wherein the step of capturing one or more lines of phase sensitive light energy data comprises: generating light energy; transmitting at least a first portion of the generated light energy onto a reference reflector wherein at least a portion of the transmitted first portion of light energy is reflected by the reference reflector; transmitting at least a second portion of the generated light energy to contact the magnetically susceptible material wherein at least a portion of the light energy that contacts the magnetically susceptible material is reflected by the magnetically susceptible material; receiving the light energy reflected by the reference reflector and by the magnetically susceptible material; combining the received light energy, wherein the received light energy interferes; and processing the combined light energy to produce the phase sensitive optical coherence data line.

33. The method of claim 32, wherein movement of the magnetically susceptible material is detected.

34. The method of claim 32, wherein the image produced has a phase sensitive resolution of at least about 30.0 nanometers (nm), 25.0 nm, 15.0 nm, 10.0 nm, 5.0 nm, 4.0 nm, 3.0 nm, or 2.0 nm.

35. The method of claim 27, wherein a plurality of phase sensitive light energy data lines are captured and used to construct the image.

36. The method of claim 35, wherein the plurality of phase sensitive light energy data lines are spatially and temporally distinct and wherein the image comprises a B-mode image frame comprising at least two of the lines.

37. The method of claim 35, wherein the plurality of phase sensitive light energy data lines are temporally distinct and wherein the image comprises a M-mode image comprising at least two of the lines.

38. The method of claim 35, wherein at least a first phase sensitive light energy data line is captured during the application of the first magnetic field strength, wherein at least a second phase sensitive light energy data line is captured during application of the second magnetic field strength, and wherein the captured lines are used to create the image.

39. The method of claim 35, wherein the first magnetic field strength has a first predetermined magnetic flux density and the second magnetic field strength has a second predetermined magnetic flux density.

40. The method of claim 39, wherein the first predetermined magnetic flux density is less than the second predetermined magnetic flux density.

41. A method for detecting a cell, comprising:

applying a first time-varying magnetic field strength to a cell, wherein the cell comprises a cellular membrane and a magnetically susceptible material and wherein the first magnetic field strength interacts with the magnetically susceptible material to induce an electrical eddy current within the magnetically susceptible material;

applying a second magnetic field strength to the cell that interacts with the induced eddy current to cause a change in the cell; and

detecting the cell by detecting the change in the cell caused by the interaction of the second magnetic field strength with the induced eddy current, wherein the change is detected using a phase sensitive frequency domain opti-

36

cal coherence tomographic imaging modality including a common path interferometer.

42. The method of claim 41, wherein the change in the cell is selected from the group consisting of: movement of the cell, movement of the magnetically susceptible material, a change in the cellular membrane tension level, and a change in the internal strain field of the cell.

43. The method of claim 41, wherein the magnetically susceptible material is non-magnetic.

44. The method of claim 43, wherein the magnetically susceptible material comprises gold, silver, or zinc.

45. The method of claim 41, wherein the magnetically susceptible material is magnetic.

46. The method of claim 41, wherein the phase sensitive optical coherence tomographic imaging modality comprises using a probe for transmitting and receiving light energy to and from the cell.

47. The method of claim 46, wherein the probe further comprises a magnetic source for applying at least one of the first and second magnetic field strengths to the cell.

48. The method of claim 41, wherein at least one of the first and second magnetic field strengths is applied to the cell from a magnetic source located external to the probe.

49. The method of claim 41, wherein the magnetically susceptible material is located within the cell.

50. The method of claim 41, wherein the magnetically susceptible material is targeted to location on the cellular membrane of the cell.

51. The method of claim 41, wherein the magnetically susceptible material comprises a plurality of metallic nanoparticles.

52. The method of claim 51, wherein the cell is detected in vivo.

53. A system for detecting a cell, comprising:

a plurality of magnets configured to apply first and second distinct magnetic field strengths to the cell, wherein the cell comprises a cellular membrane and a magnetically susceptible material, and wherein the second magnetic field strength interacts with the magnetically susceptible material to cause a change in the cell relative to interaction of the cell with the first magnetic field strength; and a phase sensitive frequency domain optical coherence tomographic imaging modality including a common path interferometer for detecting the change in the cell while it is in the presence of at least one the first and second distinct magnetic field strengths.

54. The system of claim 53, wherein the phase sensitive optical coherence tomographic imaging modality comprises using a probe for transmitting and receiving light energy to and from the cell.

55. The system of claim 54, wherein the probe further comprises at least one of the plurality of magnets.

56. The system of claim 55, wherein at least one of the plurality of magnets is located external to the probe.

57. The system of claim 53, wherein the phase sensitive optical coherence tomographic imaging modality comprises using:

a light source, a light splitter, a probe and a reference reflector, wherein light energy generated by the light source can be transmitted to and split by the splitter for transmission to the reference reflector and to the probe, wherein the probe is configured to transmit at least a portion of the light energy transmitted thereto into a target cell and to receive reflected light energy from the target cell, and wherein the reference reflector is configured to reflect at least a portion of the light energy transmitted thereto; and

37

a processor for processing reflected light energy from the reference reflector and light energy received by the probe to produce a phase sensitive optical coherence tomography image.

58. The method of claim 57, wherein the probe further comprises a single optical fiber and a rotary reflector in optical communication with the single optical fiber.

59. The system of claim 57, wherein the probe comprises the reference reflector.

60. A method for detecting a composition comprising metal, the method comprising:

applying a first magnetic field strength to the composition; applying a second magnetic field strength to the composition, wherein the second magnetic field strength is different from the first magnetic field strength and the second magnetic field strength interacts with the composition to cause a change in the composition relative to interaction of the composition with the first magnetic field strength; and

detecting the composition using a phase sensitive frequency domain optical coherence tomographic imaging modality including a common path interferometer during the application of at least one of the first and second magnetic field strengths.

61. The method of claim 60, wherein the composition is located inside of a cell and the change in the composition causes a change in the cell.

62. The method of claim 61, wherein the step of detecting the composition further includes detecting the change in the cell.

63. The method of claim 62, wherein the change in the cell that is detected is selected from the group consisting of: movement of the cell, movement of the metallic composition, a change in the cellular membrane tension level, and a change in the internal strain field of the cell.

64. The method of claim 61, wherein the composition is connected to non-cellular biological matter.

38

65. The method of claim 64, wherein the non-cellular biological matter is selected from the group consisting of: a protein, a lipid, a peptide, and a nucleic acid.

66. The method of claim 60, wherein the composition is connected to the external surface of the cellular membrane of a cell and the change in the composition causes a change in the cell.

67. The method of claim 66, wherein the step of detecting the composition further includes detecting the change in the cell.

68. The method of claim 67, wherein the change in the cell that is detected is selected from the group consisting of: movement of the cell, movement of the metallic composition, a change in the cellular membrane tension level, and a change in the internal strain field of the cell.

69. The method of claim 60, wherein the composition comprises a paramagnetic or magnetic material.

70. A method for detecting a magnetically susceptible material, the method comprising:

applying a first magnetic field strength to the magnetically susceptible material;

applying a second magnetic field strength to the magnetically susceptible material, wherein the second magnetic field strength is different from the first magnetic field strength and the second magnetic field strength interacts with the magnetically susceptible material to cause a change in the magnetically susceptible material relative to interaction of the magnetically susceptible material with the first magnetic field strength; and

detecting the magnetically susceptible material using a phase sensitive frequency domain optical coherence tomographic imaging modality including a common path interferometer during the application of at least one of the first and second magnetic field strengths.

71. The method of claim 70, wherein the magnetically susceptible material comprises a magnetic or paramagnetic material.

* * * * *